CMS Draft Analysis Note

The content of this note is intended for CMS internal use and distribution only

2014/07/01
Head Id: 248927
Archive Id: 248861:248927M
Archive Date: 2014/06/30
Archive Tag: trunk

Search for displaced photons using conversions at 8 TeV.

Alberto Ocampo, Michael Sigamani and Ward Van Driessche[2]

[1] University of Ghent
[2] CERN

Abstract

A search is performed for long-lived neutral particles decaying into a photon and invisible particles. An example of such a signature is the decay of the lightest neutralino with nonzero lifetime into a gravitino and a photon in a gauge-mediated supersymmetry model, with the neutralino as the next-to-lightest supersymmetric particle and the gravitino as the lightest. The search uses events containing photons, missing transverse energy, and jets. The impact parameter of the photon relative to the beam-beam collision point can be reconstructed using photons converting into electron/positron pairs. The data sample corresponds to an integrated luminosity of 19.3 fb^{-1} in pp collisions at $\sqrt{s} = 8$ TeV, recorded in summer of 2012 by the CMS experiment at the LHC.

1 Introduction

When looking for SUSY particles many features are model-dependent. For example, when assuming R-parity to be conserved, the Lightest SUSY Particle (LSP) is not the same in every model and thus exhibits widely different features for different models. Examples of these supersymmetry models are minimal supergravity (mSUGRA) [?], anomaly-mediated SUSY breaking (AMSB) [?], hidden valley models [?] and gauge-mediated supersymmetry breaking (GMSB) [?]. Of these heavy superparticles, some of them can be neutral. These can decay into photons and invisible particles. The former particles can interact with our detector and can therefore be detected, whereas the latter do not. The lifetime of these neutral particles is a free parameter in the model.

This anaylsis is largely based on a previous analysis performed with the 7 TeV dataset [?]. They used a conversions analysis that will be explained in more detail in section 3. Basically it comes down to choosing a model, one of the many that are possible in the world of SUSY, and look if there is an interaction (e.g. a decay) that can be examinated in the CMS-experiment. To look for an interaction, a *main search variable* has to be determined. A variable that can be constructed from experimental data and if the interaction occurs, can be distinguished from other background interactions that also give a certain non-zero value to this variable. In order to do this we first compute how the signal should look like if the interaction occurs and make sure that it can in fact be distinguished from other background interactions. If the analysis proves to be strong enough to distinguish signal from background, from our experimental data, limits can be set on the probability of an interaction of this sort to happen.

Another analysis that should be mentioned is the timing analysis done using the same 7 TeV dataset [?]. This timing analysis is different than the conversion method used here. It is a more powerful analysis as the photons do not have to convert into an e^+e^- pair. The two methods can however be combined to improve our statistics and thus yield a better result.

2 Search Channel

The SUSY model that is considered is a GMSB model and our main search variable is the transverse Impact Parameter. More specifically, we are looking at the decay as is shown in figure 1 [?].

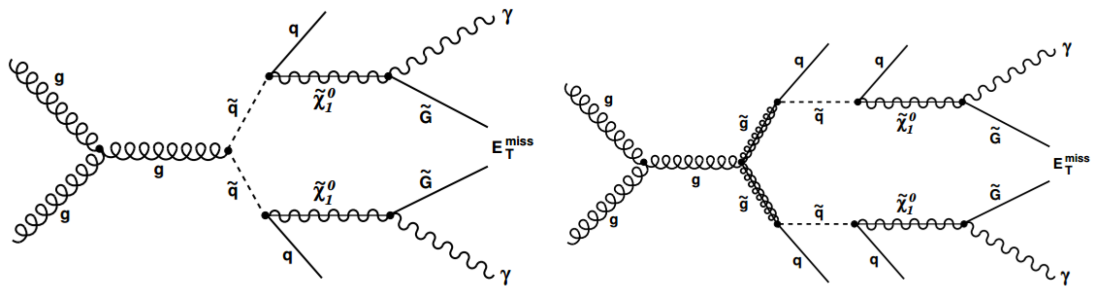

Figure 1: Feynman diagram of $\tilde{\chi}_1^0$ pair productions and $\tilde{\chi}_1^0 \to \gamma + \tilde{G}$ decay.

Here the neutralino $\tilde{\chi}_1^0$ is the Next To Lightest SUSY Particle (NLSP) while the gravitino is the Lightest SUSY Particle (LSP). We search for a signature of a photon with significant impact parameter (defined below) in association with missing transverse energy E_T^{miss} (MET) from the invisible gravitinos. Because we are assuming a conservation of R-parity, the neutralino must decay into the stable gravitino. The lifetime of the neutralino is not known (free parameter) but if we assume it to be large enough, it is possible to reconstruct photons that do not originate from the interaction vertex, signalling this SUSY event. We use photons that undergo a conversion into e^+e^- pairs in the tracker. The tracks of the electrons and positrons can be precisely reconstructed and used to calculate the photon trajectory.

The data is collected by the CMS detector at the LHC using proton-proton collisions at a center-of-mass-energy of 8 TeV in 2012. The data corresponds to an integrated luminosity of 19.3 fb^{-1}*. The analysis strategy is to start with a diphoton in the final state, then examine the impact parameter of every single photon for the displaced photon signal. E_T^{miss} and the presence of jets are also required. The result will be an upper limit to the cross section for pair-production of $\tilde{\chi}_1^0$s, each of which decays into a photon and invisible particles, and will be set as a function on $\tilde{\chi}_1^0$ lifetime of which we will generate a number of samples.

3 Photon Conversion Method: Impact Parameter

As mentioned in section 1 one must construct a main search variable. This variable is described in the following.

The CMS Tracker based on silicon technology was designed to provide robust and precise reconstruction of charged-particle momenta in the high occupancy environment of LHC collisions. This inevitably led to a substantial amount of tracker material. The direct consequence is that a large fraction of photons convert into e^+e^- pairs while traversing the tracker material. These are called *photon conversions*.

Considering the case that photons from $\tilde{\chi}_1^0$ convert into e^+e^- pairs in the CMS tracker, the photon conversion reconstruction can obtain the positions of the conversion vertices, as well as the photon directions from the e^+e^- pairs. The latter is something a regular photon reconstruction cannot. By extrapolating along the momentum direction from the conversion vertex back to the beam line, we can calculate the impact parameter of the displaced photons (figure 2). The conversion reconstruction method has already been used so far in several physics applications [?].

The transverse impact parameter d_{XY} is the distance of closest approach of the photon trajectory to the beamline in the transverse plane. It is the minimal distance a $\tilde{\chi}_1^0$ would have travelled before decaying. The longitudinal impact parameter d_{Z} is the distance from the chosen primary vertex and z position where d_{XY} is calculated (equation 1). The photon trajectory is defined as a straight line from conversion vertex along the conversion momentum.

$$
\begin{aligned}
d_{XY} &= -L_X \cdot \sin\phi + L_Y \cdot \phi \\
d_Z &= L_Z - \frac{L_X \cdot p_X + L_Y \cdot p_Y}{p_T} \cdot \frac{p_Z}{p_T}
\end{aligned}
\tag{1}
$$

where L is the vector between the conversion vertex and the primary vertex, and the ϕ angle is the polar angle of the conversion momentum vector p in azimuth, which is calculated by the vector summation of e^+e^- pair momenta at the conversion vertex.

*Link

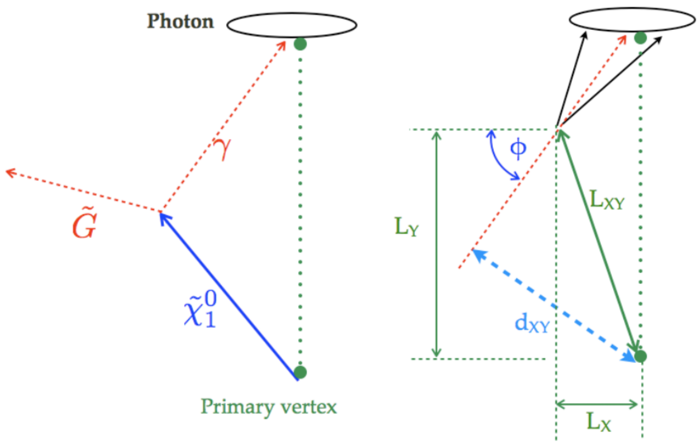

(a) (b)

Figure 2: (a): $\widetilde{\chi}_1^0 \to \gamma + \widetilde{G}$ view in the CMS tracker (b) the photon converts into e^+e^- pairs allowing to reconstruct the impact parameter.

In the high luminosity conditions, multiple collisions give multiple primary vertices. The longitudinal Impact Parameter (IP) d_Z will not be used as it has to account for this spread. We will focus on d_{XY} as the main search variable. The primary vertex is chosen by selecting the minimal χ^2-probability in every single event.

As explained above, the impact parameter (IP) of a photon (equation 1) is calculated w.r.t. the primary vertex, by extrapolating the conversion momentum from the conversion vertex. In the decay of $\widetilde{\chi}_1^0 \to \gamma + \widetilde{G}$, the non-zero IP of the photon indicates the non-zero $\widetilde{\chi}_1^0$ lifetime. The reconstructed γ d_{XY} distributions from different $\widetilde{\chi}_1^0$ lifetimes in MC samples is shown in figure 3. We see that for low $\widetilde{\chi}_1^0$ lifetimes the d_{XY} variable is not sensitive. One therefore wants to aim for longer living particles. However, if a neutralino has a very long lifetime a substantial amount of these particles will escape our detector. Therefore, only a limited range of useable neutralino lifetimes is present. The range used in this analysis runs from $c\tau = 1$ to 50 cm, where c is the speed of light and τ the lifetime.

As previously mentioned, in pile-up conditions multiple collisions give multiple primary vertices. The true primary vertex has a large divergence in the longitudinal direction, but luckily much less in the transverse direction. It is for this reason that the transverse IP and not the longitudinal IP is used in this analysis.

It should already be clear to the reader that because of the very low cross section of our signal sample it will prove to be difficult to find a region where we can distinguish signal from background. Indeed, an interaction with a low cross section inherently means that not many of these events will occur and other interations that occur much more frequently have the chance in giving non-zero contributions to our main search variable. The main reason for this is the non-perfect performance of the detector. It can occur that particles are misidentified leading to a wrong event reconstruction that can give these non-zero contributions.

The interaction that is being studied (see figure 1) will have certain physical characteristics. For example, we expect there to be multiple jets present, so removing events that have only one or zero jets will reduce the background whereas the signal will be less affected. This will be made more clear by the $n-1$ cuts in figures figures 4 and 5.

Analysis Technique This chapter begins by highlighting the physical phenomena in our events of interest in section 4. The background was estimated using a data/Monte Carlo comparison and a data-driven method which are explained in sections 5 and 6 respectively. Section 7 elaborates more on the systematic uncertainties and section 8 summarizes our results.

4 Event Selection

The data were recorded using the CMS two-level trigger system. This analysis selects events with at least two photons. A diphoton trigger is required with ECAL transverse energy thresholds E_T set to a value of 40 GeV for the leading photon. This ensures being on the plateau of the trigger efficiency, the offline analysis selects events with at least two photons in the event with $E_T > 50$ GeV.

As the previous analysis already excluded up to a Λ of 140 TeV[†], this analysis is based on a Λ-value of 180 TeV which corresponds to a lower cross section of only 0.0145 pb and a $\widetilde{\chi}_1^0$ mass of 256.8 GeV. The higher luminosity of the 2012 dataset should make it possible to probe at lower cross sections than the 2011 dataset. This means that the only remaining free variable is the $\widetilde{\chi}_1^0$ lifetime, which is determined by the parameter C_{grav}. The different lifetimes are listed in Table 1.

Table 1: List of the used χ_1^0 lifetimes in this analysis.

Λ [TeV]	$c\tau$ [cm]	σ [pb]
180	1, 5, 25, 50	0.0145

Because of the high luminosity during the run, many events had multiple proton-proton interactions (called “pile-up”), leading to a distribution of primary vertices. The pile-up conditions at high luminosity affect the event selections, in particular conversion reconstruction efficiencies. The generated pile-up distribution in the Monte Carlo samples was reweighted.

It is also notable to mention that apart from the decay into a photon $\widetilde{\chi}_1^0 \to \gamma + \widetilde{G}$ there is a corresponding decay into a Z-boson $\widetilde{\chi}_1^0 \to Z + \widetilde{G}$. The branching ratio in the GMSB model between these two is determined by the parameter Λ. We will only select events that correspond to the former decay.

In the Monte Carlo simulation, signal photons are found to be mainly in the ECAL barrel region with high transverse energy E_T. The decay model also predicts multiple reconstructed high energy jets, as well as a large value of missing transverse energy E_T^{miss}.

Because of the single γ and jets in the final state (see fig 1), the backgrounds are

- **γ-plus-jets:** a real γ together with a jet that can be mistagged as a photon.
- **QCD multi-jets:** two jets can now be mistagged as two photons. The probability of two jets to be mistagged as photons is small but because there is such a huge QCD-event production, the background is substantial enough te be taken into account.
- **$t\bar{t}$-jets:** the top quark can decay semileptonically ($t \to Wb \to l\nu_l b$) and the lighter lepton is mistagged as a photon together with a jet being misinterpreted as a photon. We expect this background to be neglegible.

[†]More information can be found in section ??.

We have to select our events in such a way that we cut away as much background as possible while leaving the highest amount of signal. This is illustrated in the so-called $n-1$ plots in figures 4 and 5. $n-1$ plots show the distribution of a variable where all the cuts (n) are implemented except for the cut on the concerned variable ($n-1$). Although, because we are dealing with very low statistics in our analysis, the cut on the number of photons is discarded. The signal sample used has a lifetime with $c\tau = 50$ cm.

The unconverted and converted photon candidates are reconstructed from clusters of energy in the ECAL. At least one photon candidate with transverse $E_T > 50$ GeV and reconstructed in the ECAL barrel region is required. The transverse distribution of energy in the associated cluster of ECAL crystals must be consistent with that expected from a photon, and the energy detected in the HCAL behind the photon shower cannot exceed 5% of the ECAL energy. Events originating from decaying heavy particles as the ones we are looking for are characterised by isolated photons. To look for these isolated photons, we use official CMS search criteria. We look at a cone around the photon with a $\Delta R < 0.3$ ($\Delta R = \sqrt{(\Delta\eta)^2 + (\Delta\phi)^2}$) (see figure 6). The pseudorapidity η is a variable that indicates if the particle in question is travelling in a direction perpendicular to the beam, in parallel or something in between. It is defined as:

$$\eta = -\ln\left[\tan\left(\frac{\theta}{2}\right)\right] \tag{2}$$

where θ is the polar angle with respect to the counter clockwise beam direction and goes from 0 (perpendicular) to ∞ (longitudinal).

The following photon isolation criteria are used to select these "good photons":

- $\sum E_T^{\text{Charged hadron}} < 2.6$ GeV
- $\sum E_T^{\text{Neutral hadron}} < 3.5 + 0.04 \cdot E_T^{\text{Central photon}}$ GeV
- $\sum E_T^{\text{Other photons}} < 1.3 + 0.004 \cdot E_T^{\text{Central photon}}$ GeV
- $\sigma_{i\eta i\eta} < 0.012$;
- $H/E < 0.05$;

where H/E has been defined as the sum of the energies of HCAL towers within a cone of size $\Delta R < 0.15$ centred on the supercluster position, divided by the supercluster energy[‡]. $\sigma_{i\eta i\eta}$ is a measure of the transverse profile of the shower.

In the ideal situation, two to four jets are expected for neutralino pair-production as illustrated in figure 1. However, considering the jet reconstruction efficiency and energy resolution, at least two jets with $\eta \leq 2.4$ with $p_T > 35$ GeV are required.

If a $\tilde{\chi}_1^0 \rightarrow \gamma + \tilde{G}$ decay were to occur, one expects a γ that signals a rather large impact parameter together with large E_T^{miss} from the invisible $\tilde{G}$. So, as already explained frequently in this analysis, E_T^{miss} is an important parameter indicating the difference between signal and background. As is motivated in the 7 TeV analysis [**?**], a cut of $E_T^{miss} > 30$ GeV for the signal selection is set in order to eliminate most of the background and keep the signal efficiency.

Because it is possible that an electron deposits its energy in the calorimeter and fakes either

[‡] More information can be found in this link.

a photon or a conversion, these events are now be vetoed out with the help of some well chosen cuts. We motivate this choice with the help of figure 7. It is clear that when we veto the events where a conversion or a photon matches an electron, these background events will reduce as many more electrons fake a conversion or a photon in the $t\bar{t}$-jets background (this is also the reason why it is a background). The figure shows that the ratio of this matching to no matching is much higher for the $t\bar{t}$-jets background than for the signal sample. Therefore, more background than signal events will be vetoed out.

5 Data/MC comparison

For a first background determination, we started by trying to get a data/Monte Carlo (MC) comparison. The agreement should not be perfect because the QCD/γ+jets modelling are known to be sub-optimal and the QCD MC statistics are also very low. This is illustrated in figures 8 to 12. S_{Minor} is the minor axis of the ellipse from the energy deposit in the ECAL. $\sigma_{i\eta i\eta}$ is a measure of the transverse profile of the shower. Its properties are used to ensure that the candidate is consistent with the shape expected from a photon.

From these figures we see that the data/MC comparison is far from ideal but it's the best we could do. However, some important conclusions can be made:

- The main backgrounds are not well modelled in Monte Carlo.
- The γ+jets is our main background and the QCD-jets and $t\bar{t}$-jets are almost negligible.
- The E_T^{miss} does not depend on the $\tilde{\chi}_1^0$-lifetime (which is expected).
- The signal region is in the high E_T^{miss} tail.

The main search variable d_{XY} is shown in figure 12. These results were presented to the Long Lived group in CMS. Because we encountered the need of at least two photons in our events, one of the comments was to try the di-photon trigger instead of the single photon trigger that was used up to now. This would allow us to lower the thresholds on the photon p_T and give us more useful data. Essentially this meant for us to change the code to run on AOD (Analysis Object Data) instead of RECO (Reconstructed data).

6 Background Determination

We can see from figures 8 to 12 that the MC does not model the data very well. This is both due to a lack of MC statistics and known mis-modelling effects (for QCD and γ+jets) due to large uncertainties on the cross section etc. However, they are reasonable enough to conclude that our key variables are understood both in data and MC. For $t\bar{t}$-bar, since this is a negligible background (less than 1%), we estimate this using MC scaled to luminosity. For γ+jets we estimate the shape and normalisation using a data driven approach, which will be explained in this section.

The data-driven background determination is a strategy for estimating the QCD and γ+jets background via data control samples that are kinematically similar to the candidate sample while having no real E_T^{miss} (remember that this parameter is expected to be high in the signal region). In the main backgrounds, the single-γ-plus-jets events and QCD mulit-jets events, the jets can be misidentified as photons and are called *fake photons*. These fake photons have to fail at least one of the photon isolation requirements that are given in section 4.

Indeed, the $\widetilde{\chi}_1^0 \to \gamma + \widetilde{G}$ decay has two signatures: E_T^{miss} from $\widetilde{G}$ and large transverse IP from the displaced photons. Therefore the $\widetilde{\chi}_1^0$ signal has large E_T^{miss}, while the main background (single γ-plus-jets and QCD multi-jets) has small E_T^{miss} with tails extending to high E_T^{miss}. We construct a control region of low E_T^{miss} and use this control region to estimate the background in the search/signal region, by measuring the d_{XY} distribution. Summarized, we get:

1. The background is more prominent than the signal in the region of low E_T^{miss}.
2. The data in the region of low E_T^{miss} is therefore made up almost entirely of background events.
3. The background should not depend on the E_T^{miss} as no prominent invisible particles are involved.
4. The data is separated into a background region (with low E_T^{miss}) and a signal region (with high E_T^{miss}).
5. The data in the background region can be used in the signal region because of 3.

In this analysis, we define $E_T^{\text{miss}} < 20$ GeV as the background control region, and the $E_T^{\text{miss}} > 30$ GeV as the signal region. In figure 13 we can see that, with a proper normalization, background events (fake photons) do not depend on the E_T^{miss} (point 3 in the above). Control regions 1 and 2 have similar shapes. We can also see that data in the low E_T^{miss} region can be used to estimate the background in the signal region. The background is normalized to the total number of events in the data sample.

After performing the validation checks for the data-driven method we used this estimation for figures 14 to 16. The background in the d_{XY} variable was scaled using the peak of the distribution in data. This is necessary to be non-biased for possible signal events in the tail.

The full cut flow is summarized in table 2. We clearly see that we start with a huge number of background with only a handful of signal events. The preselection includes several requirements such as a well defined interaction vertex, photons in the barrel region and photon isolation. The E_T^{miss} differentiates between the signal region ($E_T^{miss} > 30$ GeV) and background region ($E_T^{miss} < 20$ GeV). When we select the number of photons that are necessary, other photon isolation requirements are also implemented.

The final plot of the d_{XY} conversion variable is shown in figure 17 (*right*). Accounting for possible fluctuations in the data no excess in the tail is seen.

Table 2: Cutflow table of two signal samples with $c\tau = 50$ and 1 cm, the data-driven, $t\bar{t}$-bar and total background, the signal-over-background ratio and the data. We assumed systematic uncertainties of 10% for signal and 30% for the background.

	GMSB (180,50)	GMSB (180,1)	Bkg.[DD]	TTJet	Total Bkg	$\frac{S}{\sqrt{B}}$	Data
All	280 ± 28	280 ± 28	$2.2 \cdot 10^{12}$	$2.6 \cdot 10^{5}$	$(2.2 \pm 0.7) \cdot 10^{12}$	$2 \cdot 10^{-4}$	$2.2 \cdot 10^{12}$
Presel.	174 ± 17	179 ± 18	$7.1 \cdot 10^{10}$	$8.5 \cdot 10^{3}$	$(7.2 \pm 2.2) \cdot 10^{10}$	$2 \cdot 10^{-4}$	$7.2 \cdot 10^{10}$
E_T^{miss} *	171 ± 17	177 ± 18	$5 \cdot 10^{10}$	$7.7 \cdot 10^{3}$	$(5.0 \pm 1.5) \cdot 10^{10}$	$8 \cdot 10^{-4}$	$5.0 \cdot 10^{10}$
No. jets≥ 2	92 ± 9	95 ± 10	$3.2 \cdot 10^{9}$	$3.9 \cdot 10^{3}$	$(3.2 \pm 1) \cdot 10^{9}$	$2 \cdot 10^{-3}$	$2.1 \cdot 10^{9}$
No. $\gamma \geq 2$	40 ± 4	40 ± 4	$2.1 \cdot 10^{7}$	0.02	$(2.1 \pm 0.6) \cdot 10^{7}$	0.01	$1.3 \cdot 10^{7}$
No. conv.≥ 1	4 ± 0.4	6 ± 0.6	40	0.02	40 ± 12	0.58	43

*We differentiate between the signal region ($E_T^{miss} > 30$ GeV) and background region ($E_T^{miss} < 20$ GeV).

7 Systematic Uncertainties

The uncertainty in the luminosity determination is 2.2 % [?]. The sources of systematic uncertainty affecting the signal acceptance are the following. The calorimeter response to different types of particles is not perfectly linear and hence corrections are made to properly map the measured jet energy deposition. The uncertainty on this correction is referred to as the uncertainty on the jet energy scale and varies as a function of position and transverse momentum of the jet. A similar uncertainty on the photon energy scale in the barrel is also present. Due to time constraints there was not enough time to compute all the systematic uncertainties. Therefore we made an educated assumption on the systematic uncertainty (10%) and the background (30%). These uncertainties are propagated unto table 2 and figures 14 to 17. These uncertainties will be computed properly in the near future.

8 Results and Interpretation

The observed event yield in data is consistent with the SM background prediction, and upper limits are obtained on the production cross section of a long-lived neutralino in the context of the the SPS8 model of GMSB supersymmetry, assuming $\mathcal{B}\left(\tilde{\chi}_1^0 \rightarrow \gamma\widetilde{G}\right) = 100\%$. Exclusion limits are computed with a modified frequentist CL_s method [? ? ?]§, using the asymptotic approximation for the test statistic as described in reference [?]. These results are shown in figures 18, where we used a cut and count approach, and 19, where we used the asymptotic shape analysis. The latter resulted in a greater sensitivity. Figure 19 also shows that we are not sensitive for very low and very high values of $c\tau$, which is explained in more detail in section 3. The 7 TeV analysis used $\Lambda = 100$ TeV, corresponding to higher cross sections. Comparing our final result with the 7 TeV analysis (figure ??) we see that we have upper limits that are sensitive to lower cross sections.

Conclusion and Outlook

The way to search for signals of new physics as predicted by theory models, such as supersymmetry, is not clear-cut. The reason for this is the multidimensional nature of these theories. Depending on the specific combination of model parameters, the predicted signal can look quite different. It is for this reason that experimental physicists often choose a certain signal model provided by their theoretical counterpart as the base for their search. Every model has its own specifics and characteristics. Even when we have chosen a model, there is no clear cut way to optimize our analysis. The search for SUSY is not easy as we have to search for everything/anything.

In this analysis we performed a search for long-lived particles decaying into photons produced in association with jets. The photons then convert into e^+e^--pairs where we reconstruct the impact parameter d_{XY}. This is our main discriminating variable to differentiate signal to background. We used LHC proton-proton collision data at a center-of-mass energy of 8 TeV corresponding to an integrated luminosity of 19.3 fb^{-1}. We interpret our analysis using a SUSY model with a GMSB scenario with a long-lived neutralino decaying to a photon and a grav-

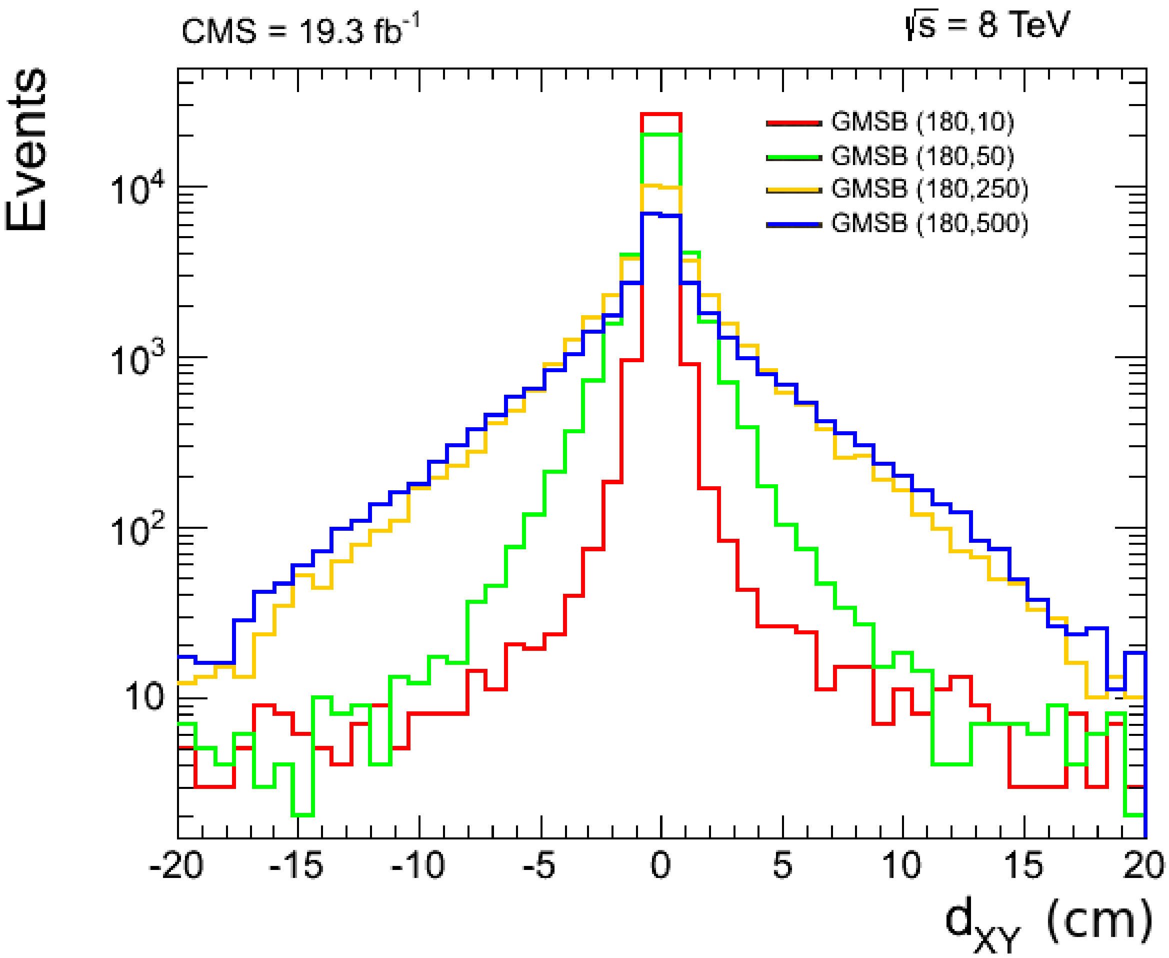
CMS = 19.3 fb^{-1}
$\sqrt{s}$ = 8 TeV
Events
GMSB (180,10)
GMSB (180,50)
GMSB (180,250)
GMSB (180,500)
d_{XY} (cm)

8cm
(a) h

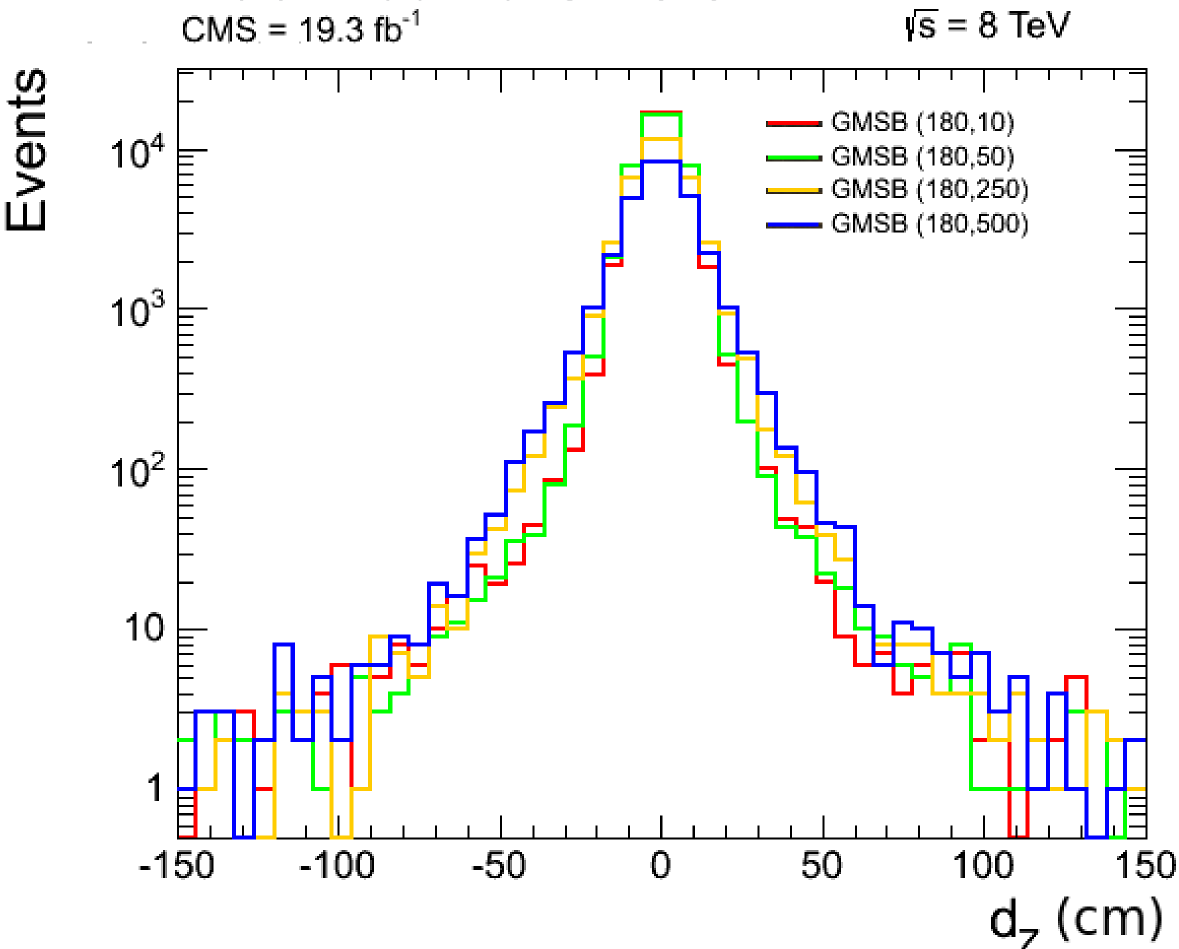
CMS = 19.3 fb^{-1}
$\sqrt{s}$ = 8 TeV
Events
GMSB (180,10)
GMSB (180,50)
GMSB (180,250)
GMSB (180,500)
d_Z (cm)

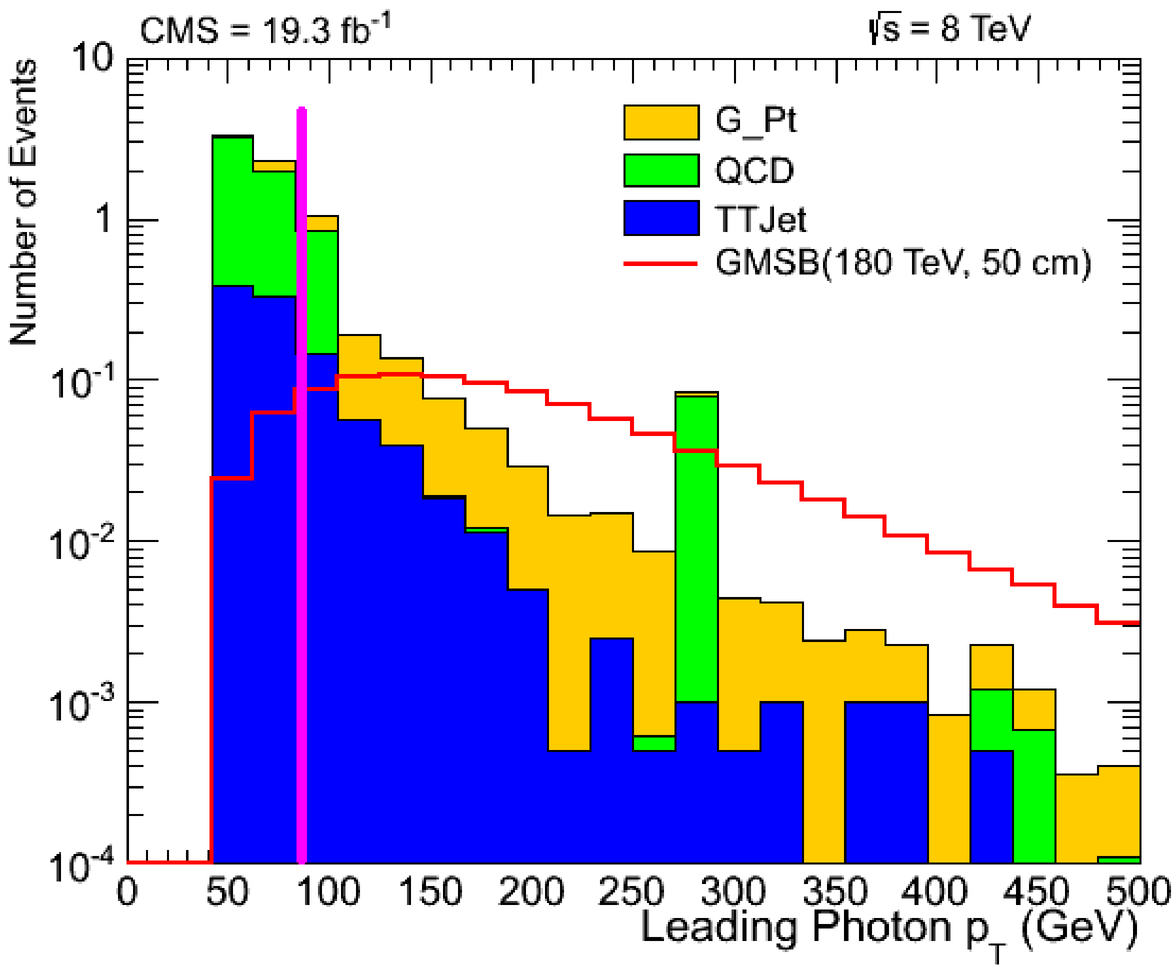
CMS = 19.3 fb^{-1}
$\sqrt{s}$ = 8 TeV
Number of Events
G_Pt
QCD
TTJet
GMSB(180 TeV, 50 cm)
Leading Photon p_T (GeV)

8cm
(a) h

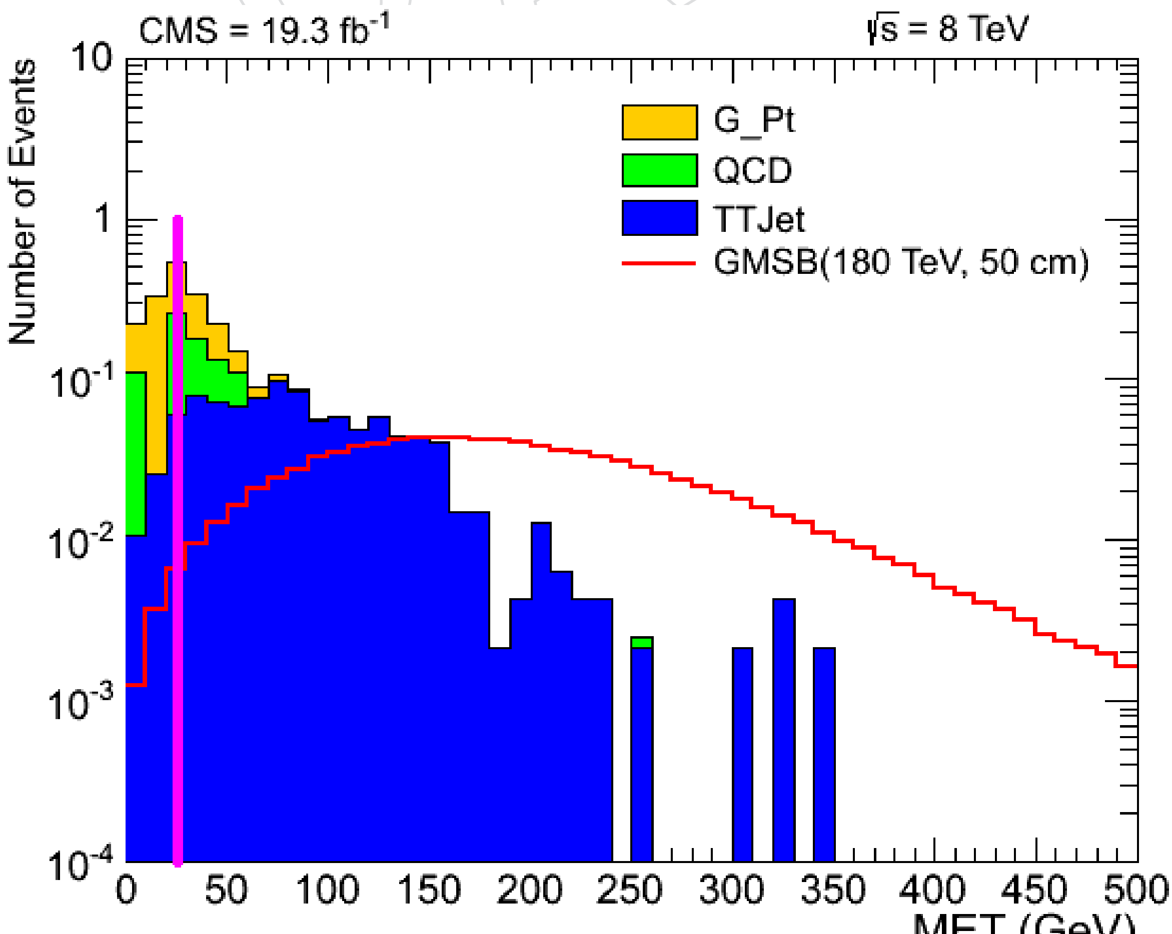
CMS = 19.3 fb^{-1}
$\sqrt{s}$ = 8 TeV
Number of Events
G_Pt
QCD
TTJet
GMSB(180 TeV, 50 cm)
MET (GeV)

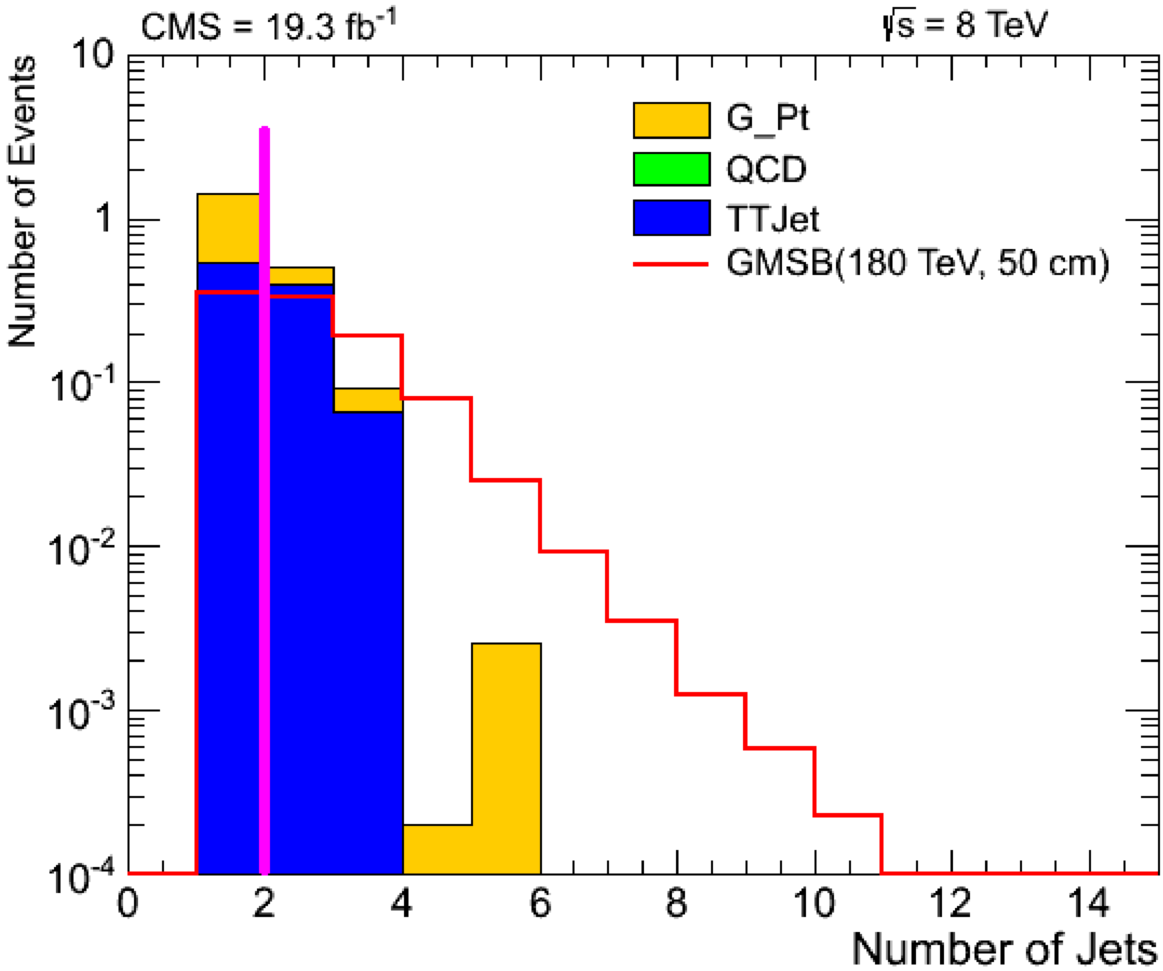
CMS = 19.3 fb^{-1}
$\sqrt{s}$ = 8 TeV
Number of Events
G_Pt
QCD
TTJet
GMSB(180 TeV, 50 cm)
Number of Jets

8cm
(a) h

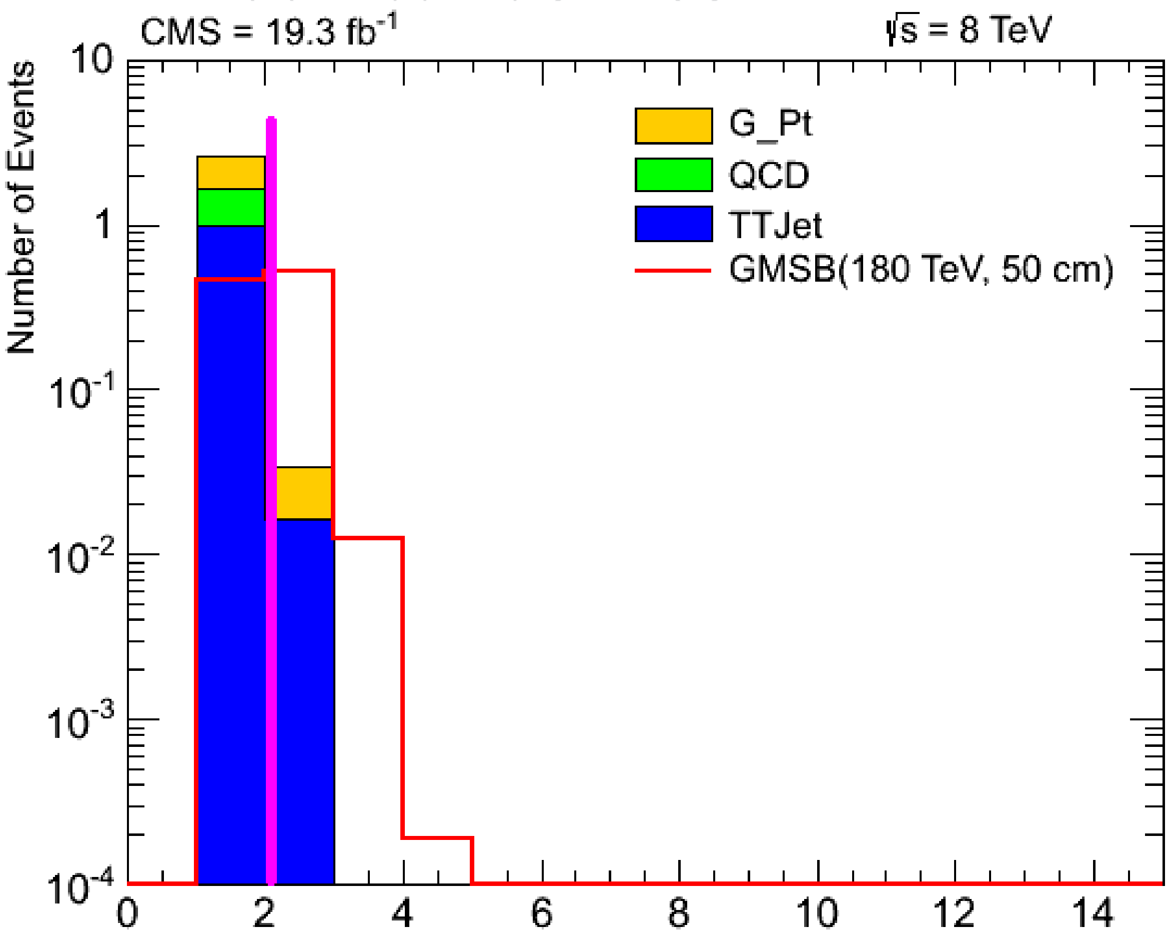
CMS = 19.3 fb^{-1}
$\sqrt{s}$ = 8 TeV
Number of Events
G_Pt
QCD
TTJet
GMSB(180 TeV, 50 cm)

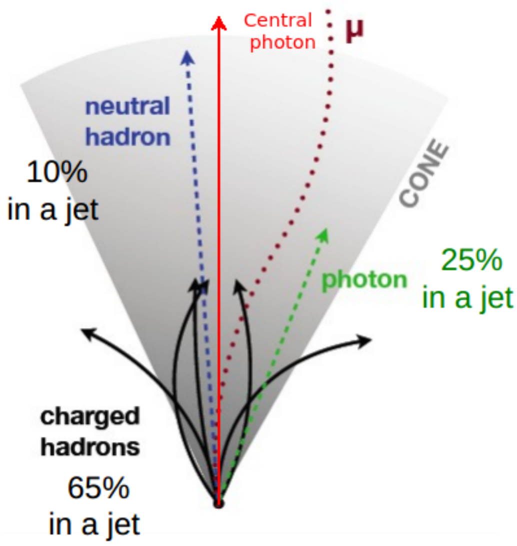

Figure 6: Example of particles that can accompany a photon. We look at particles that are close to the photon, within a cone-like shape.

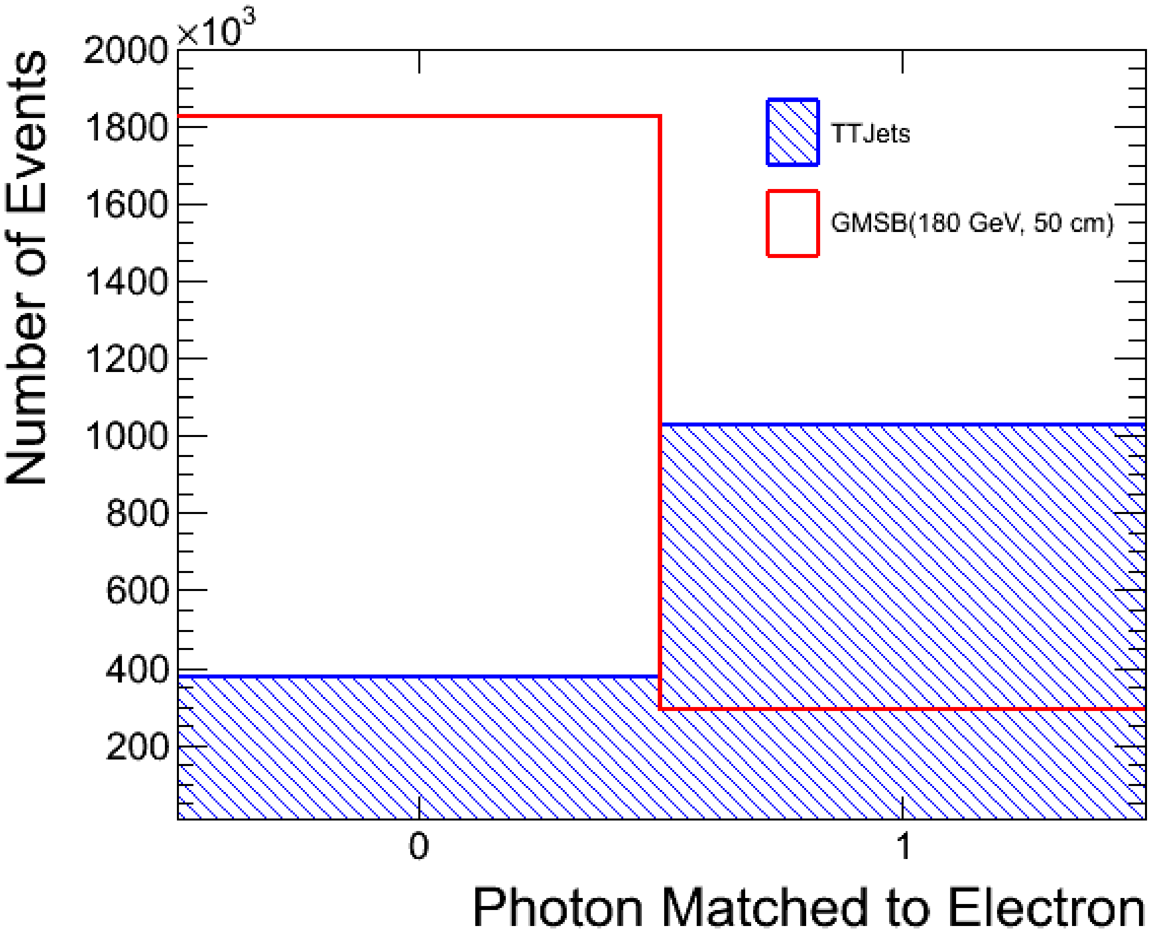
×10^3
Number of Events
2000
1800
1600
1400
1200
1000
800
600
400
200
0
1
TTJets
GMSB(180 GeV, 50 cm)
Photon Matched to Electron

8cm
(a) h

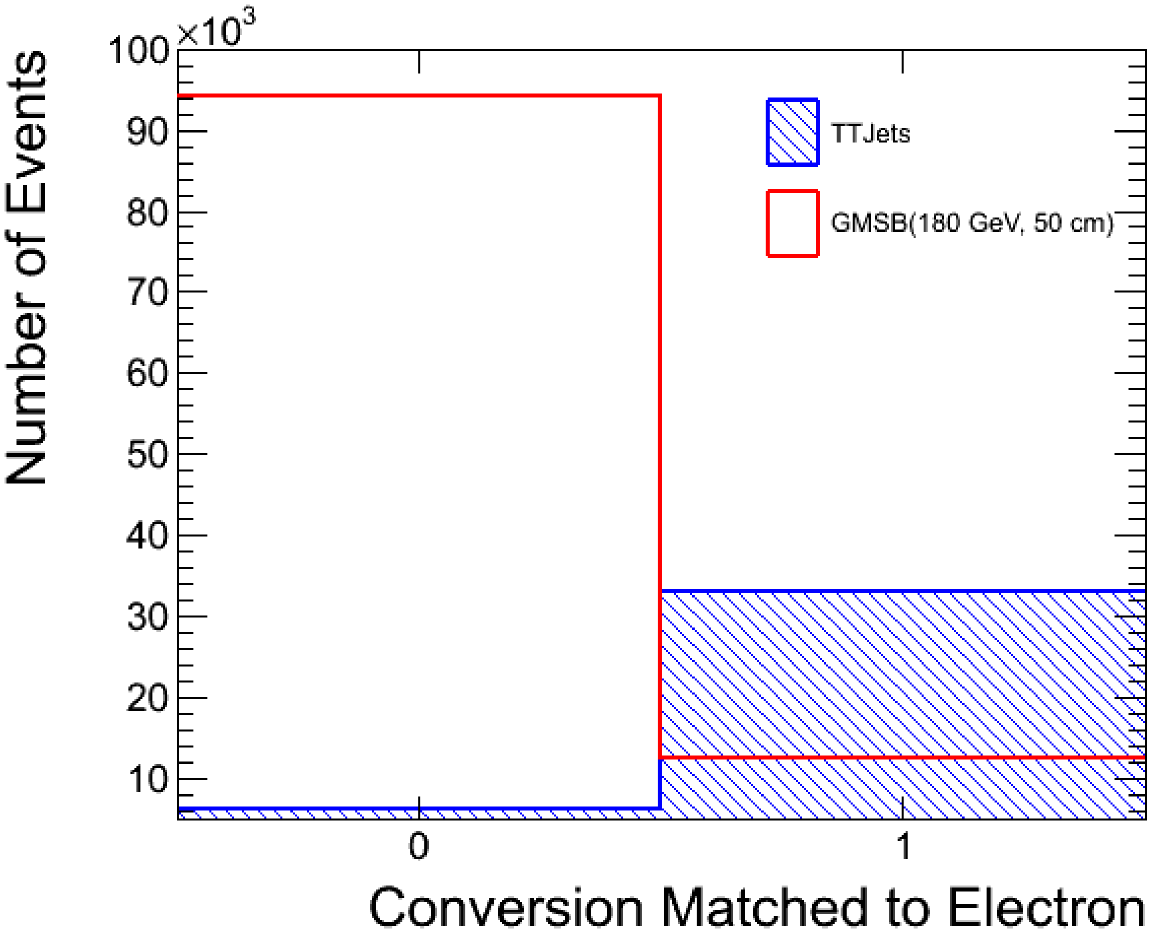
×10^3
Number of Events
100
90
80
70
60
50
40
30
20
10
0
1
TTJets
GMSB(180 GeV, 50 cm)
Conversion Matched to Electron

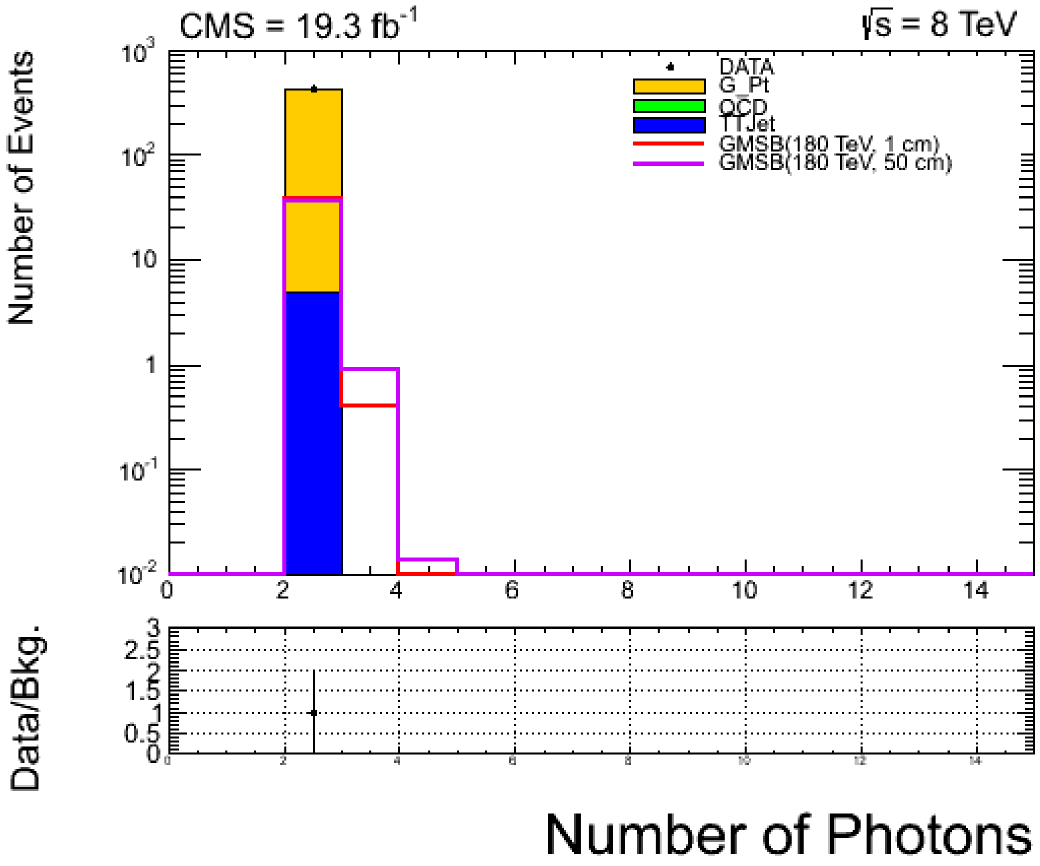
CMS = 19.3 fb^{-1}
$\sqrt{s}$ = 8 TeV
Number of Events
DATA
G_Pt
QCD
TTJet
GMSB(180 TeV, 1 cm)
GMSB(180 TeV, 50 cm)
Data/Bkg.
Number of Photons

8cm
(a) h

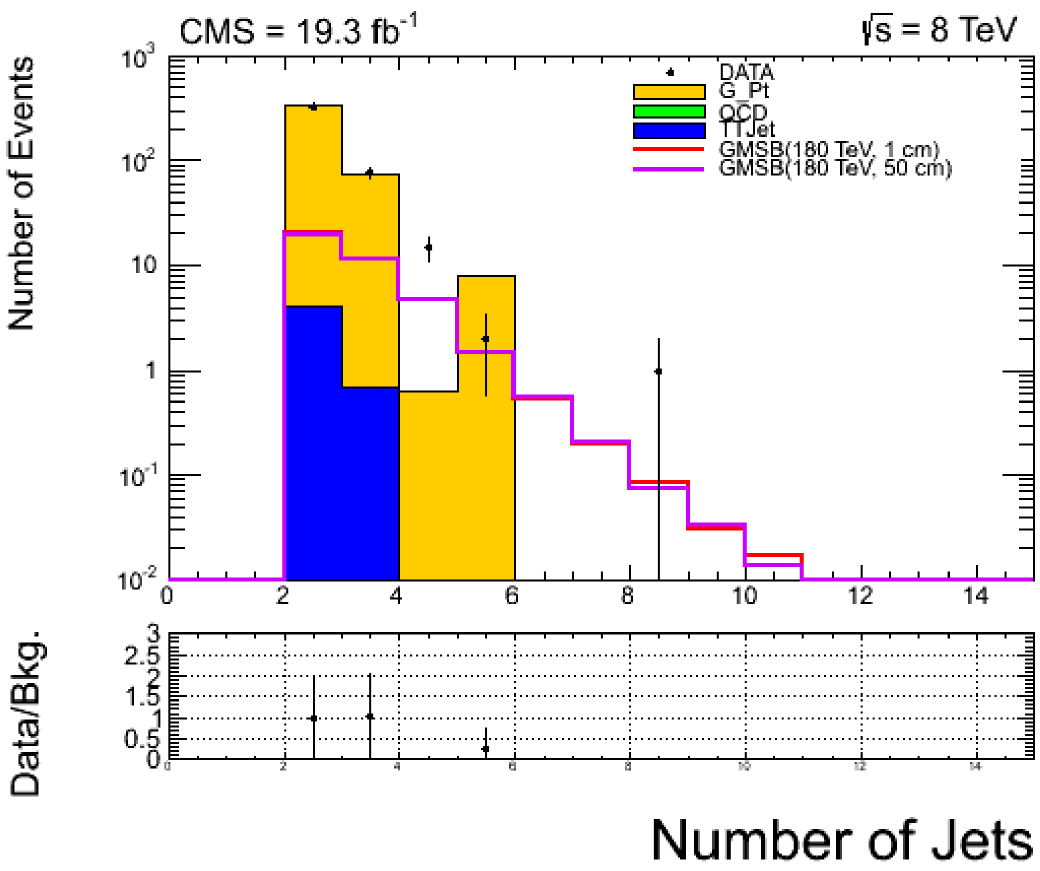
CMS = 19.3 fb^{-1}
$\sqrt{s}$ = 8 TeV
Number of Events
DATA
G_Pt
QCD
TTJet
GMSB(180 TeV, 1 cm)
GMSB(180 TeV, 50 cm)
Data/Bkg.
Number of Jets

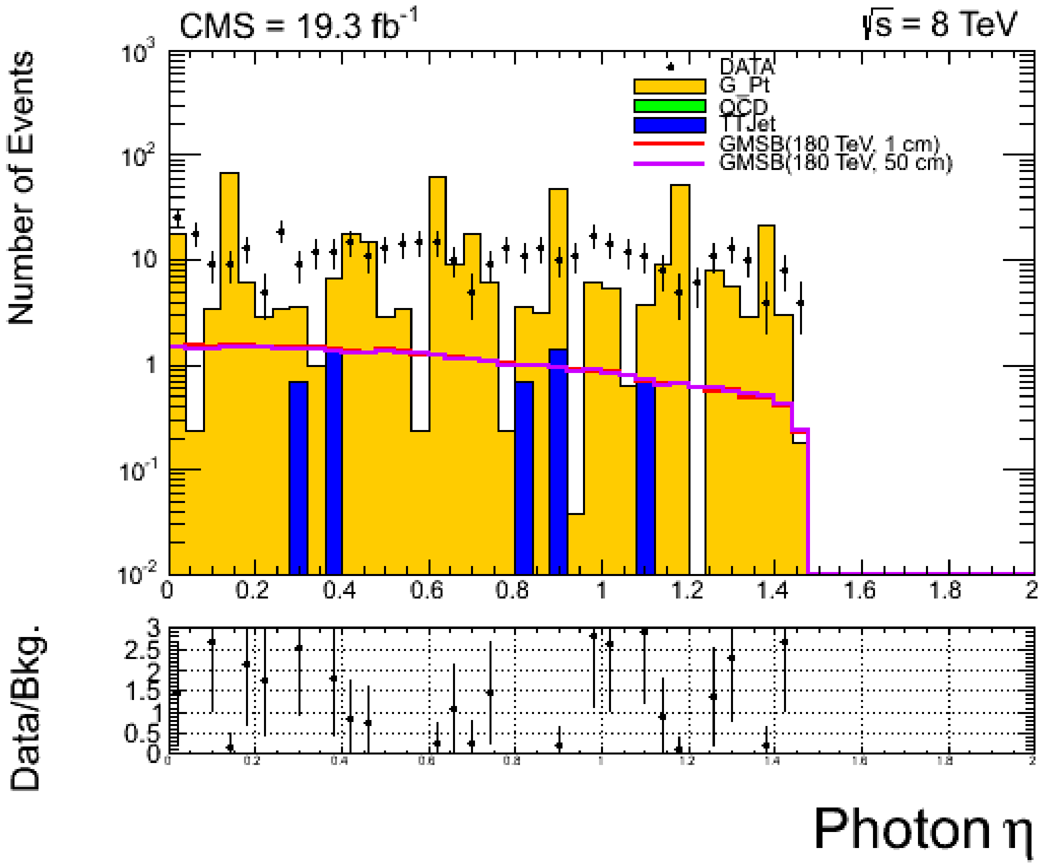
CMS = 19.3 fb^{-1}
$\sqrt{s}$ = 8 TeV
DATA
G_Pt
QCD
TTJet
GMSB(180 TeV, 1 cm)
GMSB(180 TeV, 50 cm)
Number of Events
Data/Bkg.
Photon η

8cm
(a) h

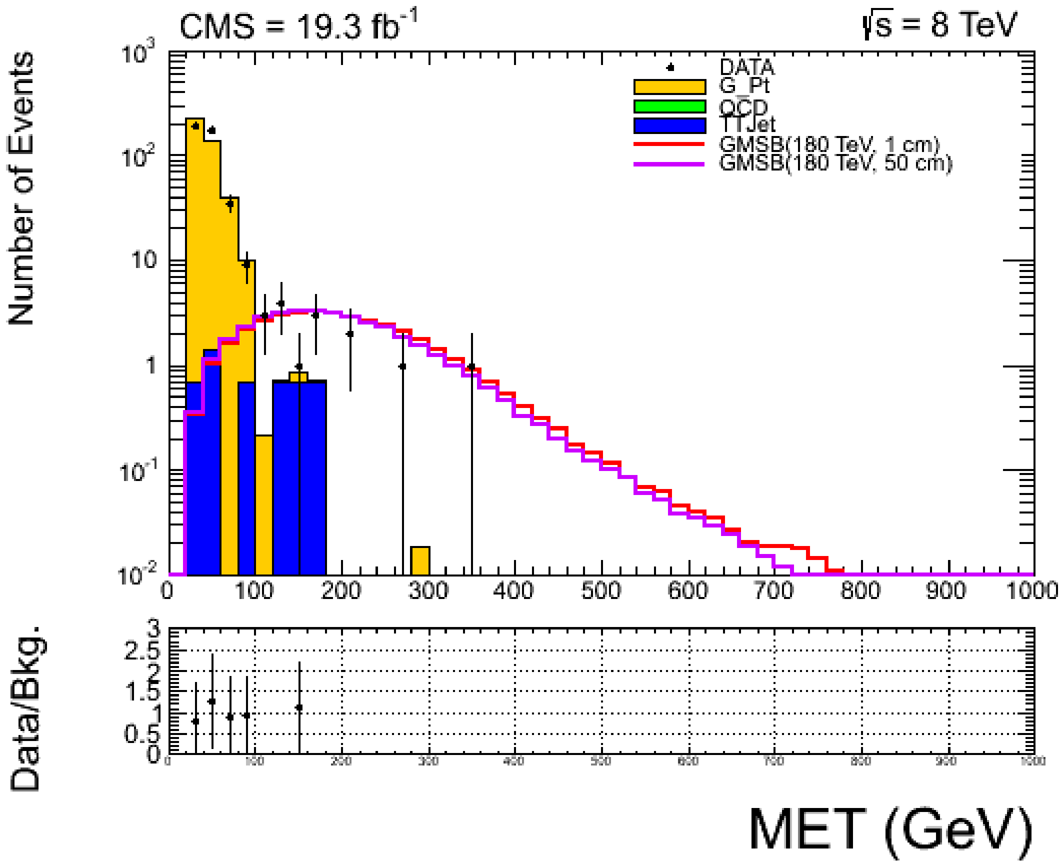
CMS = 19.3 fb^{-1}
$\sqrt{s}$ = 8 TeV
DATA
G_Pt
QCD
TTJet
GMSB(180 TeV, 1 cm)
GMSB(180 TeV, 50 cm)
Number of Events
Data/Bkg.
MET (GeV)

8

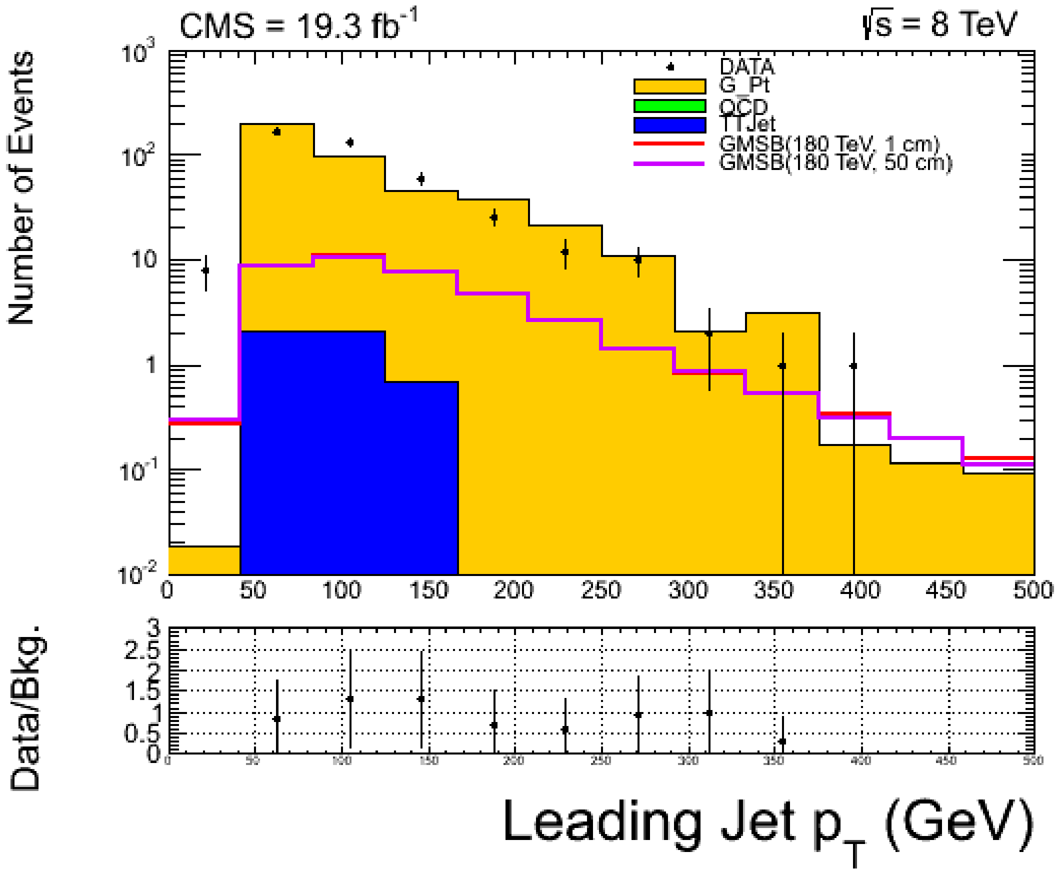
CMS = 19.3 fb^{-1}
$\sqrt{s}$ = 8 TeV
DATA
G_Pt
QCD
TTJet
GMSB(180 TeV, 1 cm)
GMSB(180 TeV, 50 cm)
Number of Events
Data/Bkg.
Leading Jet p_T (GeV)

8cm
(a) h

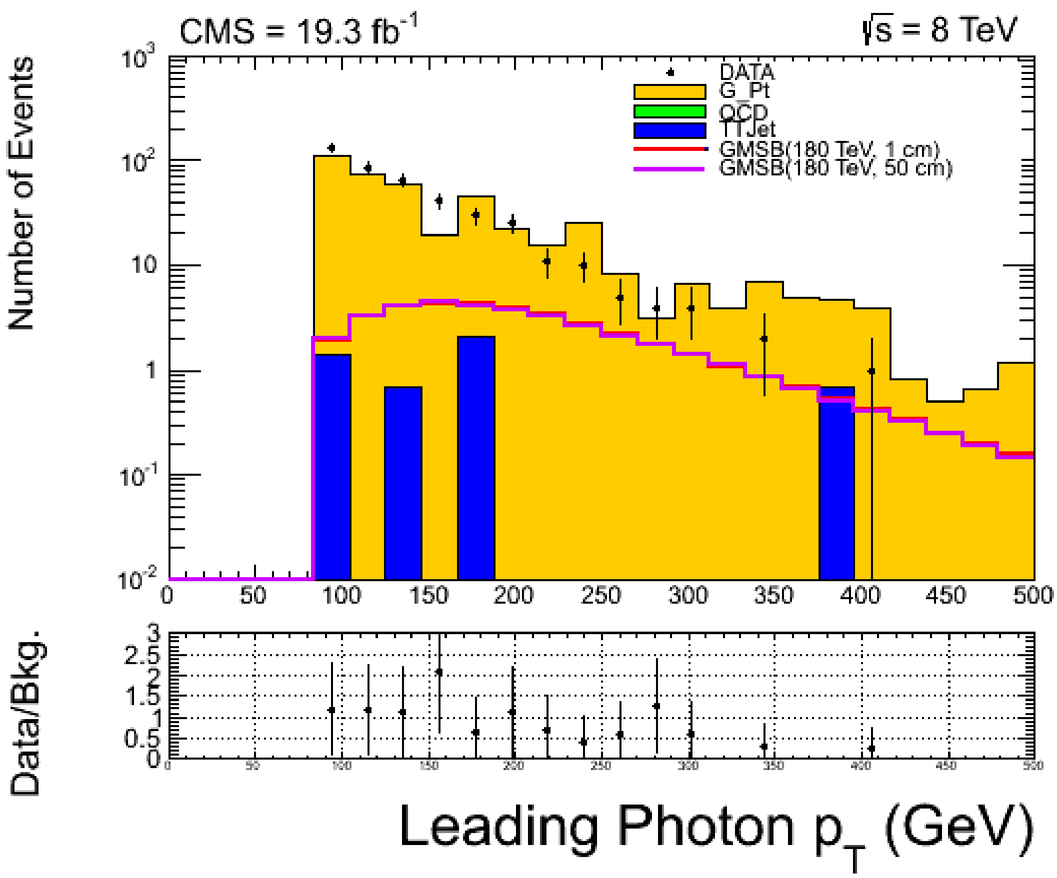
CMS = 19.3 fb^{-1}
$\sqrt{s}$ = 8 TeV
DATA
G_Pt
QCD
TTJet
GMSB(180 TeV, 1 cm)
GMSB(180 TeV, 50 cm)
Number of Events
Data/Bkg.
Leading Photon p_T (GeV)

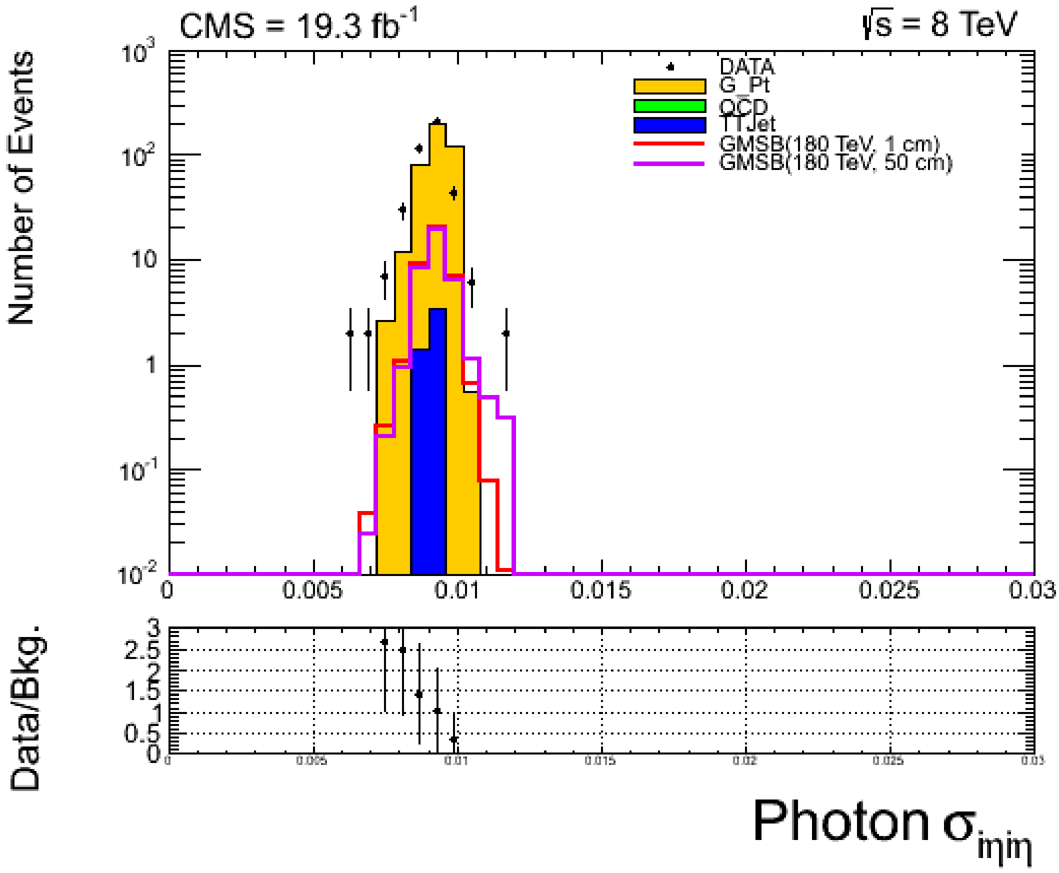
CMS = 19.3 fb^{-1}
$\sqrt{s}$ = 8 TeV
Number of Events
DATA
G_Pt
QCD
TTJet
GMSB(180 TeV, 1 cm)
GMSB(180 TeV, 50 cm)
Data/Bkg.
Photon $\sigma_{i\eta i\eta}$

8cm
(a) h

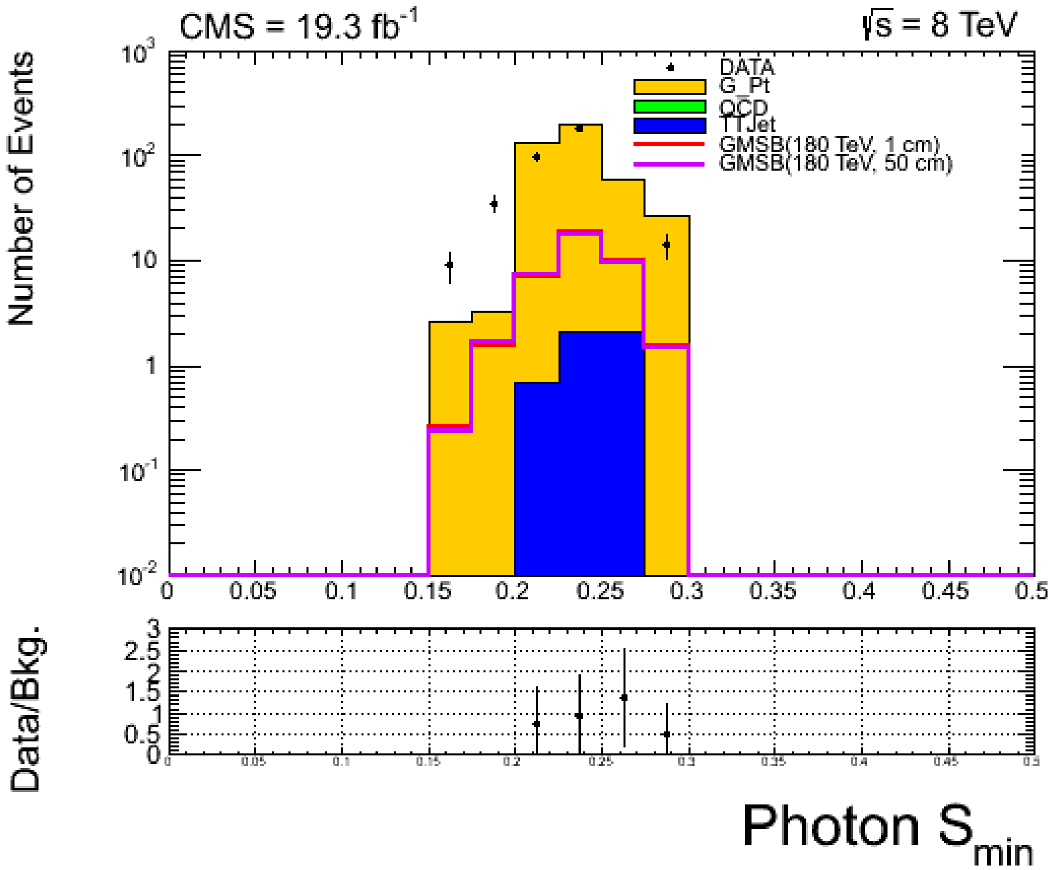
CMS = 19.3 fb^{-1}
$\sqrt{s}$ = 8 TeV
Number of Events
DATA
G_Pt
QCD
TTJet
GMSB(180 TeV, 1 cm)
GMSB(180 TeV, 50 cm)
Data/Bkg.
Photon S_{min}

8

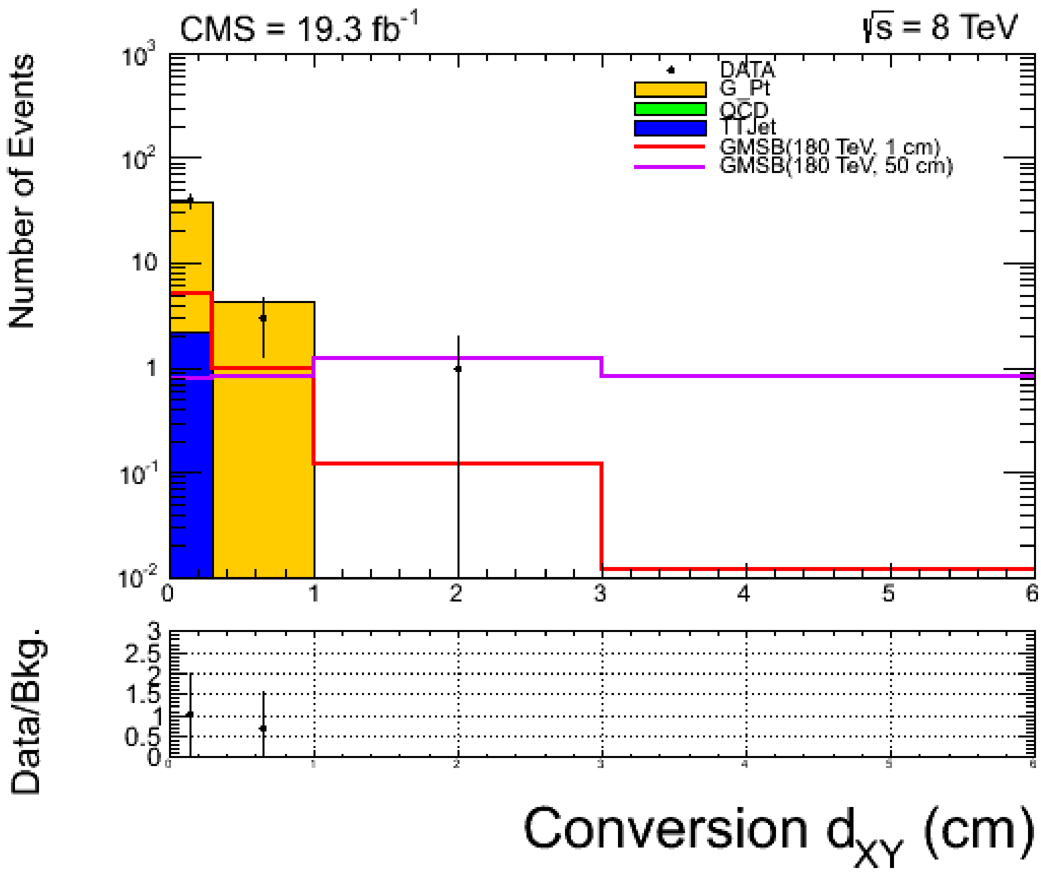

Figure 12: Data/MC comparison for d_{XY}. Two signal samples with $\Lambda = 180$ TeV and $c\tau = 1$ and 50 cm are also shown.

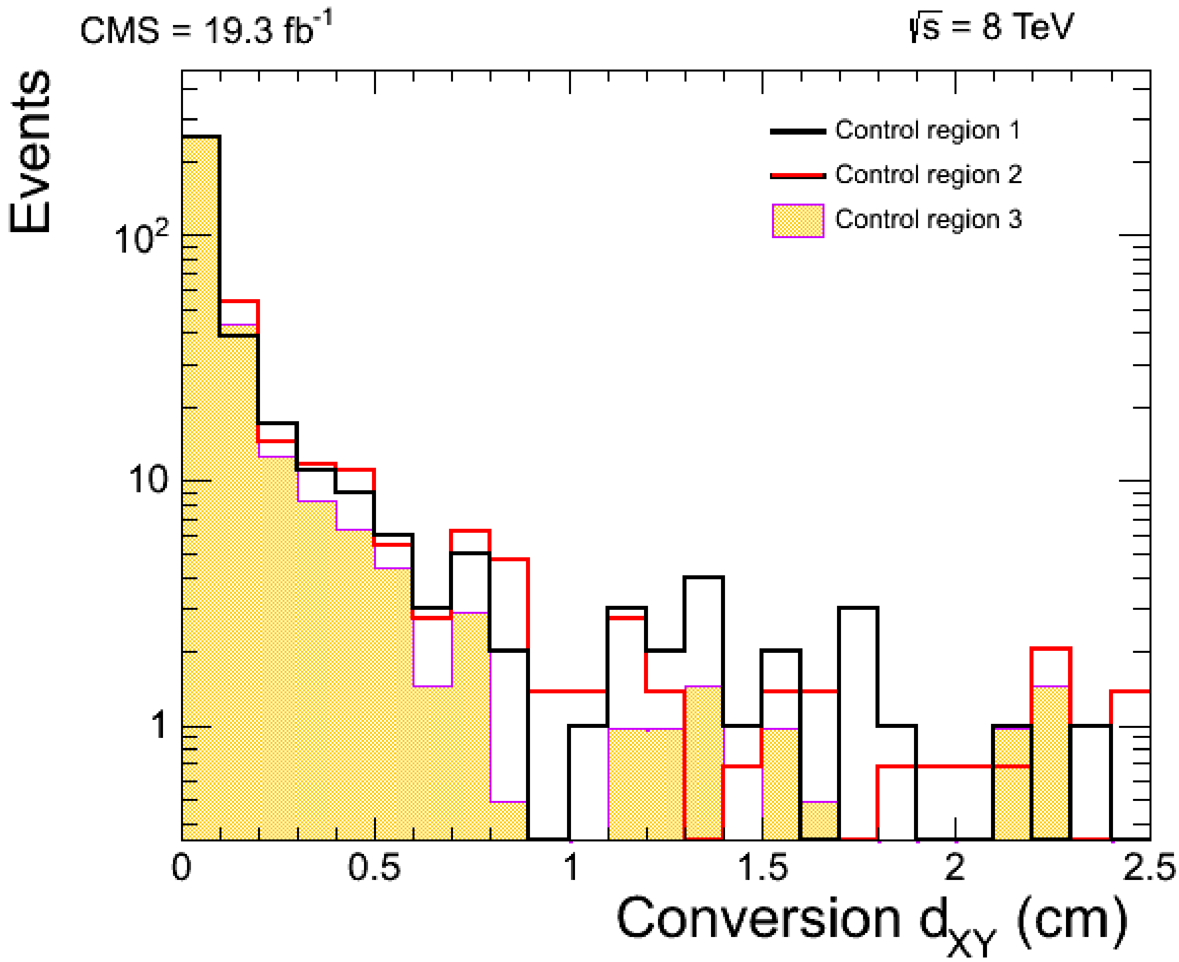

Figure 13: The shape of the fake photons (real background) in the high E_T^{miss} (control region 1) is the same as the shape of fake photons in the low E_T^{miss} (control region 2) and as the shape of real photons in the the low E_T^{miss} (control region 3).

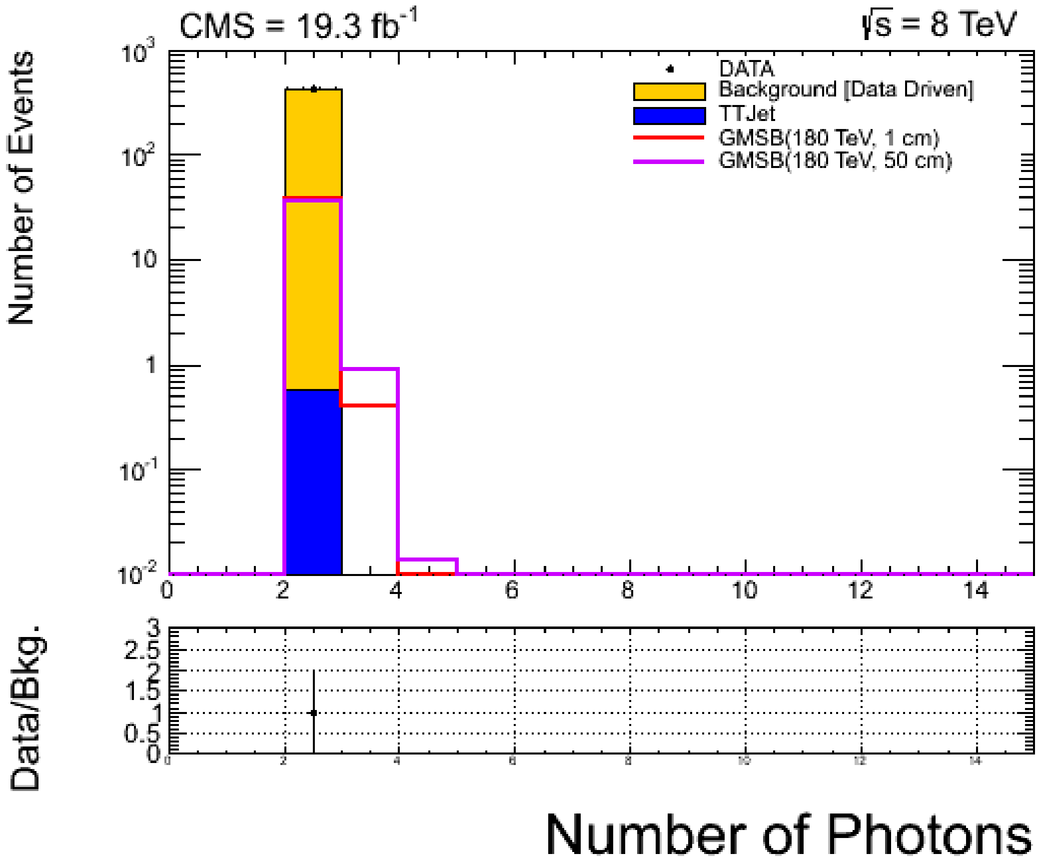
CMS = 19.3 fb^{-1}
$\sqrt{s}$ = 8 TeV
DATA
Background [Data Driven]
TTJet
GMSB(180 TeV, 1 cm)
GMSB(180 TeV, 50 cm)
Number of Events
Data/Bkg.
Number of Photons

8cm
(a) h

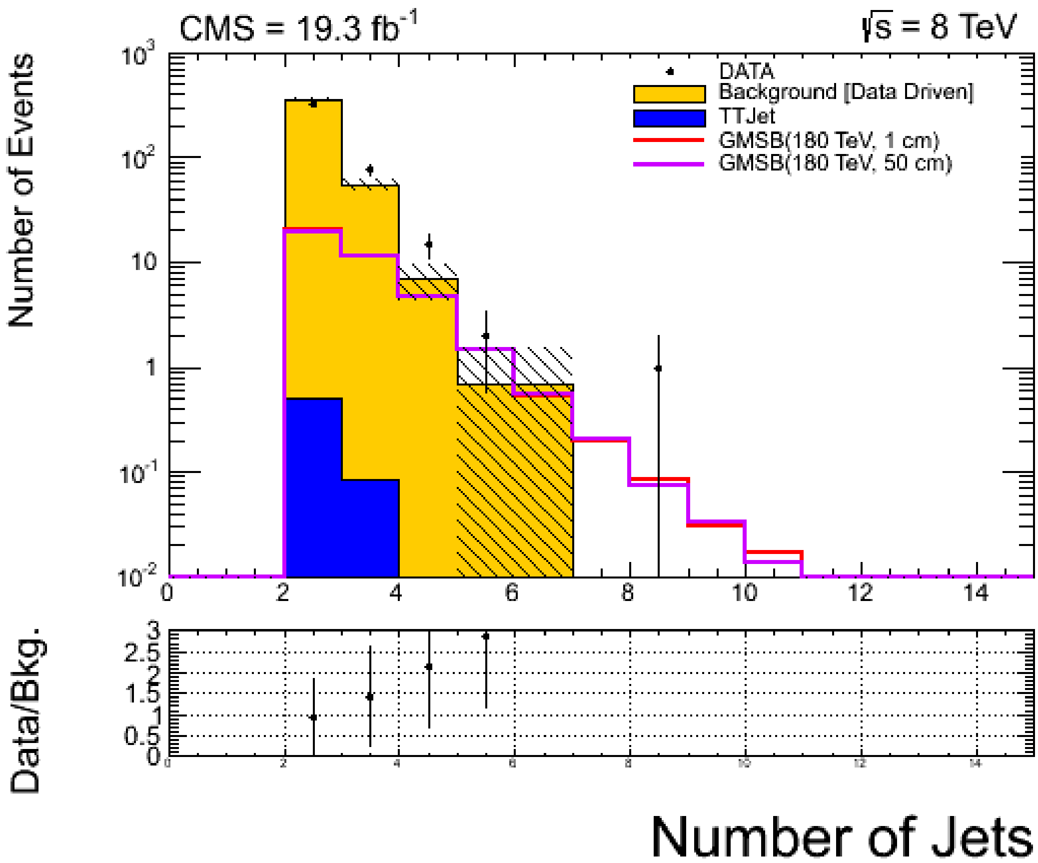
CMS = 19.3 fb^{-1}
$\sqrt{s}$ = 8 TeV
DATA
Background [Data Driven]
TTJet
GMSB(180 TeV, 1 cm)
GMSB(180 TeV, 50 cm)
Number of Events
Data/Bkg.
Number of Jets

8

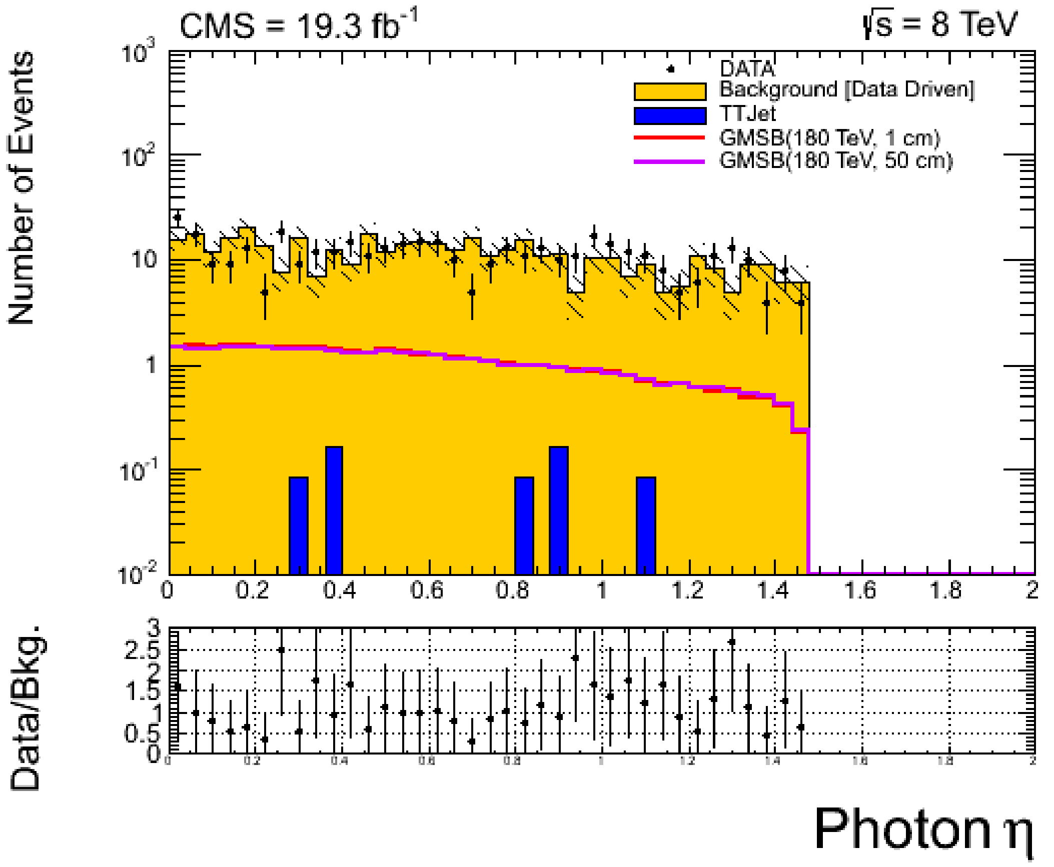
CMS = 19.3 fb^{-1}
$\sqrt{s}$ = 8 TeV
DATA
Background [Data Driven]
TTJet
GMSB(180 TeV, 1 cm)
GMSB(180 TeV, 50 cm)
Number of Events
Data/Bkg.
Photon η

8cm
(a) h

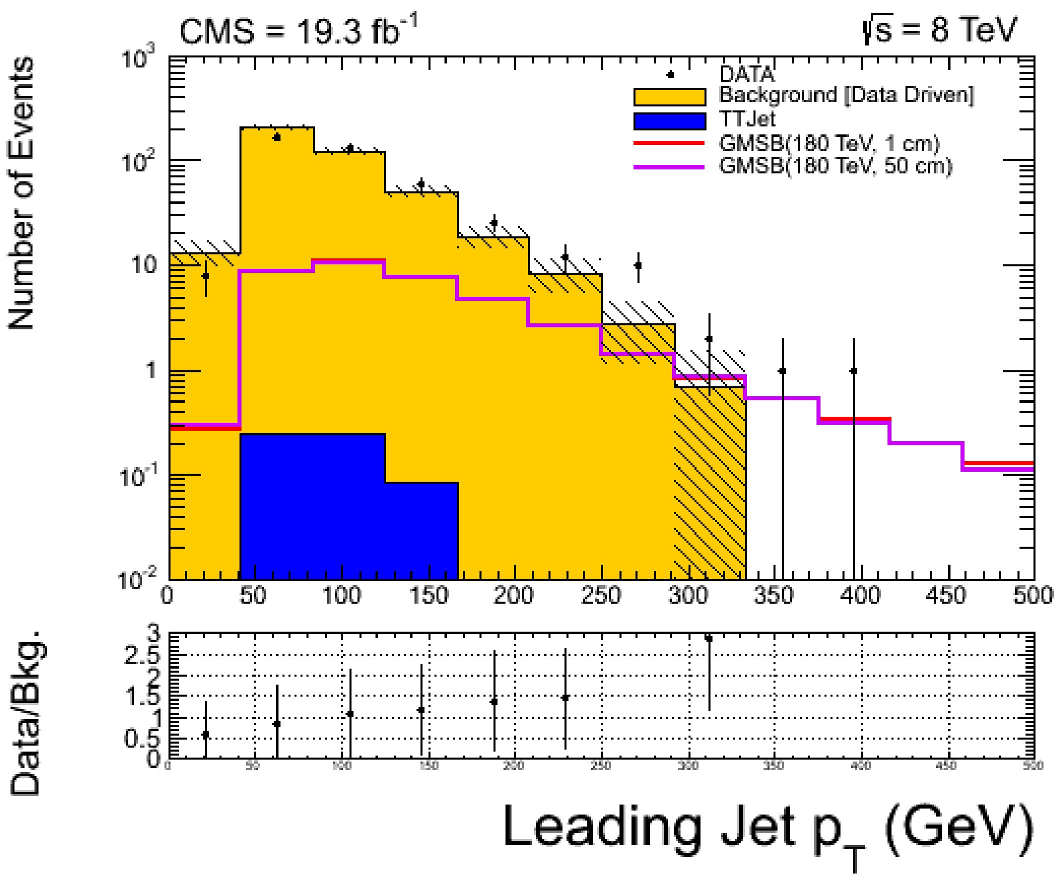
CMS = 19.3 fb^{-1}
$\sqrt{s}$ = 8 TeV
DATA
Background [Data Driven]
TTJet
GMSB(180 TeV, 1 cm)
GMSB(180 TeV, 50 cm)
Number of Events
Data/Bkg.
Leading Jet p_T (GeV)

8

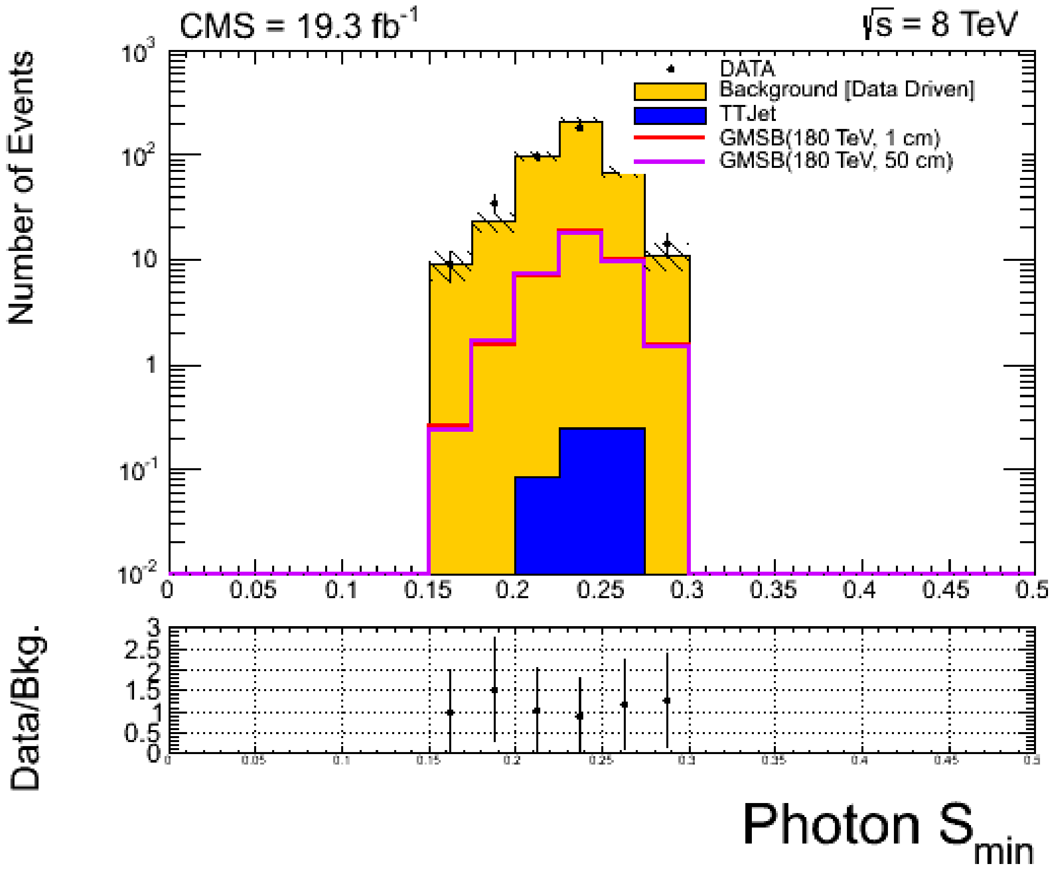
CMS = 19.3 fb^{-1}
$\sqrt{s}$ = 8 TeV
DATA
Background [Data Driven]
TTJet
GMSB(180 TeV, 1 cm)
GMSB(180 TeV, 50 cm)
Number of Events
Data/Bkg.
Photon S_{min}

8cm
(a) h

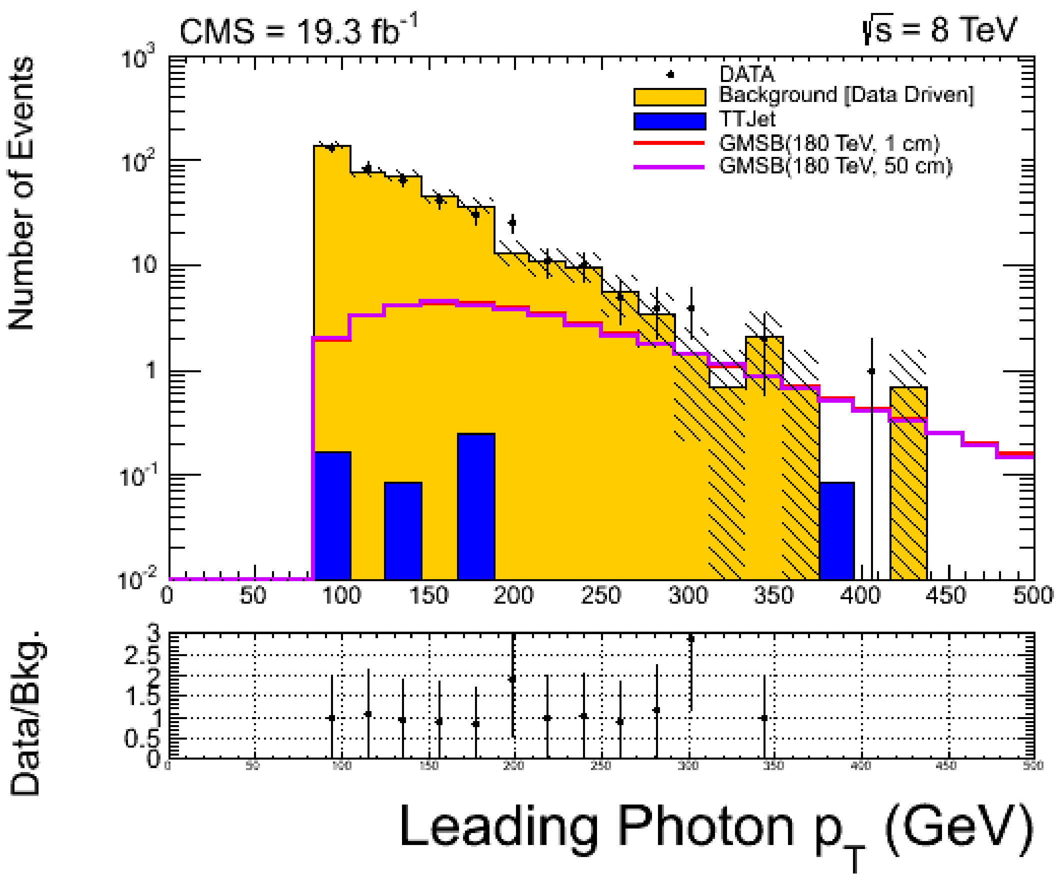
CMS = 19.3 fb^{-1}
$\sqrt{s}$ = 8 TeV
DATA
Background [Data Driven]
TTJet
GMSB(180 TeV, 1 cm)
GMSB(180 TeV, 50 cm)
Number of Events
Data/Bkg.
Leading Photon p_T (GeV)

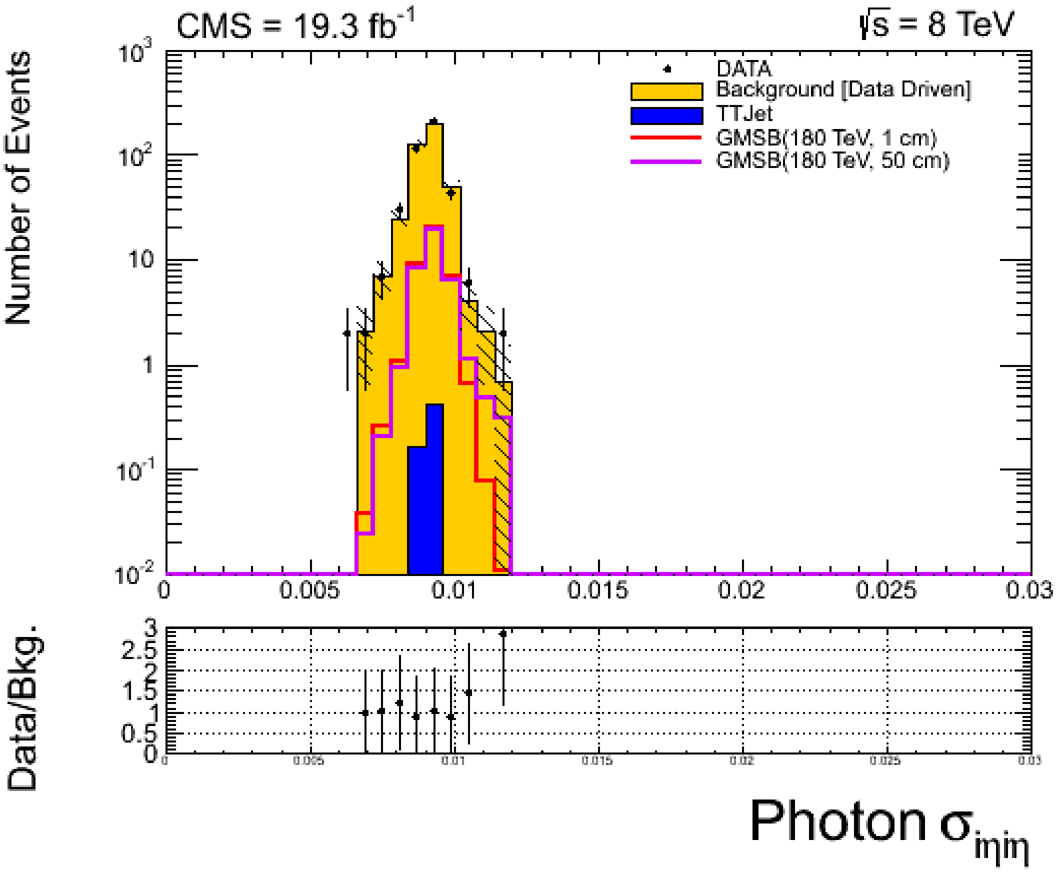
CMS = 19.3 fb^{-1}
$\sqrt{s}$ = 8 TeV
DATA
Background [Data Driven]
TTJet
GMSB(180 TeV, 1 cm)
GMSB(180 TeV, 50 cm)
Number of Events
Data/Bkg.
Photon $\sigma_{i\eta i\eta}$

8cm
(a) h

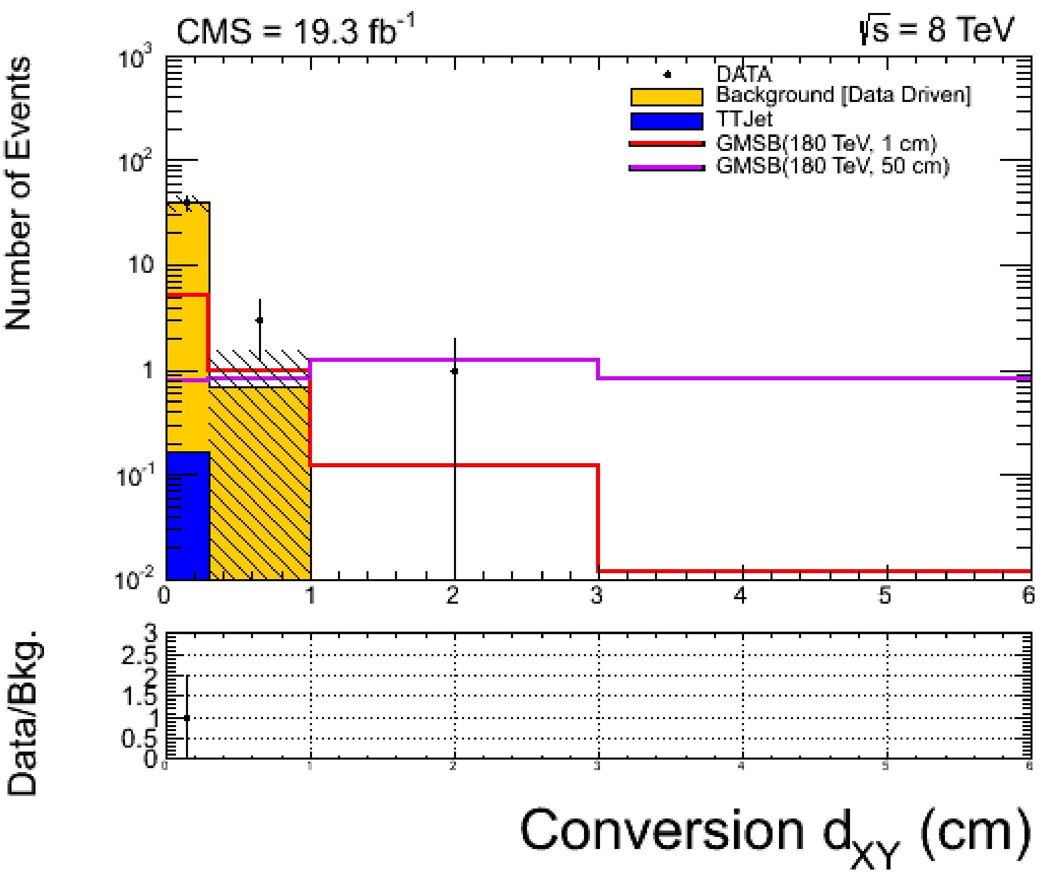
CMS = 19.3 fb^{-1}
$\sqrt{s}$ = 8 TeV
DATA
Background [Data Driven]
TTJet
GMSB(180 TeV, 1 cm)
GMSB(180 TeV, 50 cm)
Number of Events
Data/Bkg.
Conversion d_{XY} (cm)

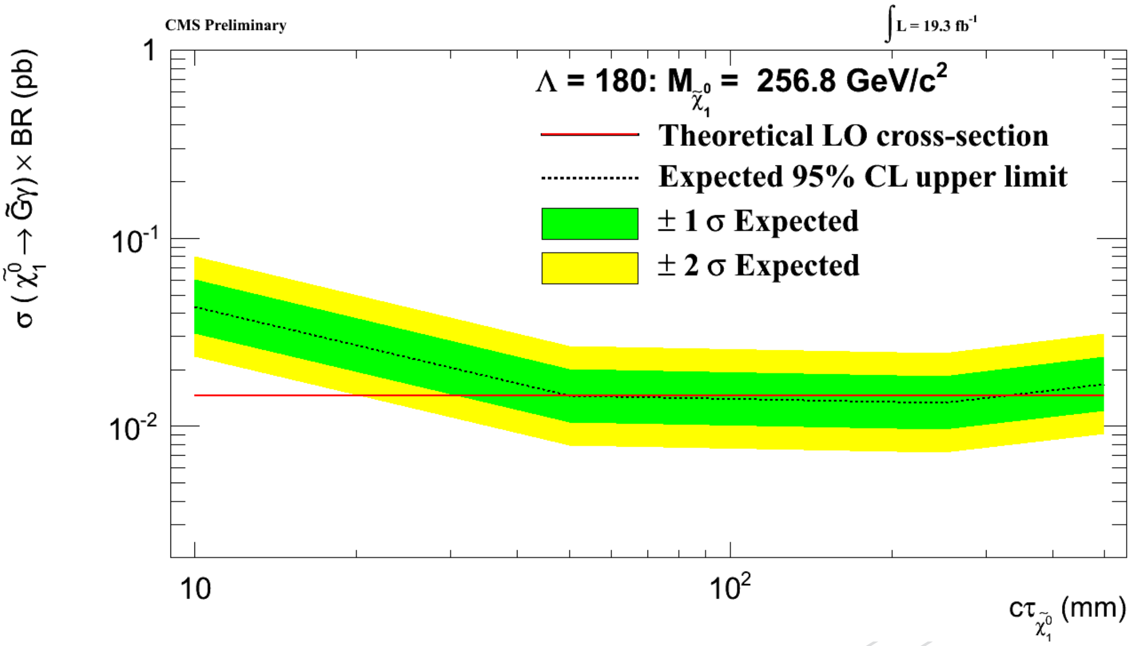

Figure 18: Cut and count expected limit plot. The expected values as a function of the $\tilde{\chi}_1^0$ proper decay length are shown by the dashed line. It indicates the expected median of results for the background-only hypothesis, while the green and yellow bands indicate the ranges that are expected to contain 68% and 95% of all observed excursions from the median, respectively. A cut on the $d_{XY} > 0.3$ cm optimizes the signal-over-background ratio. The expected limit plots are shown together with the theoretical cross section line.

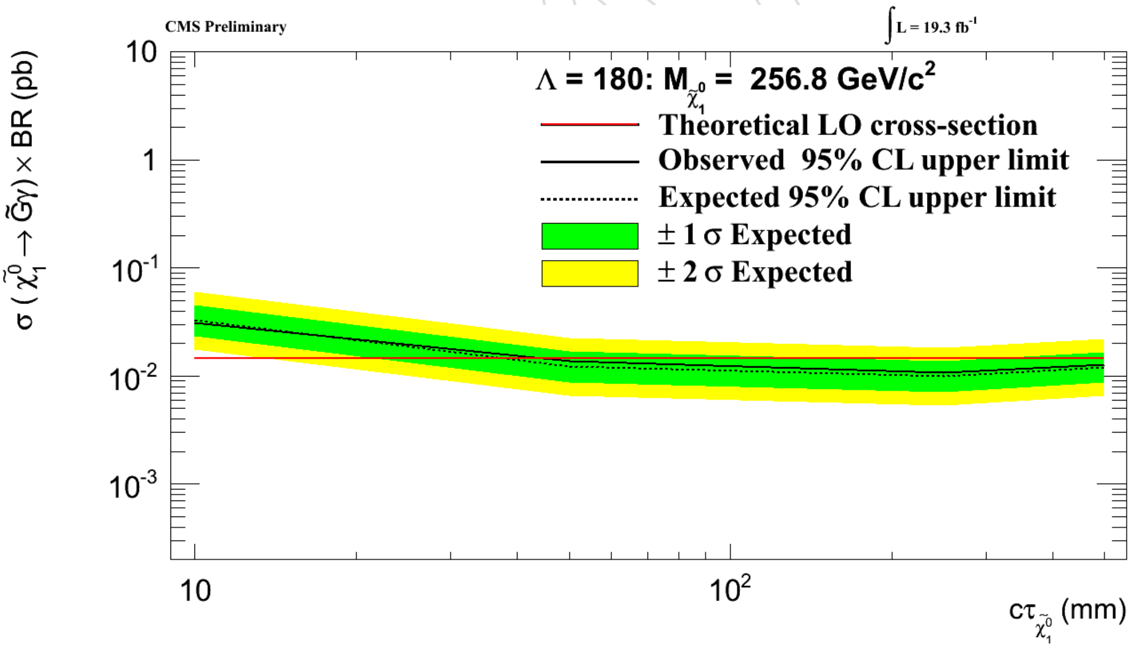

Figure 19: Shape experiment for limit plots. The observed values as a function of the $\tilde{\chi}_1^0$ proper decay length are shown by the solid line. The dashed line indicates the expected median of results for the background-only hypothesis, while the green and yellow bands indicate the ranges that are expected to contain 68% and 95% of all observed excursions from the median, respectively. This analysis not only looks at the absolute values of the d_{XY} variable, but also at its shape in the signal, background and data samples.